NATIONAL UNIVERSITY OF SCIENCE AND TECHNOLOGY POLYTECHNIC BUCHAREST

FACULTY OF BIOTECHNICAL SYSTEMS ENGINEERING

DOCTORAL SCHOOL OF BIOTECHNICAL SYSTEMS ENGINEERING

DOCTORATE THESIS SUMMARY

Studii şi cercetări privind comportarea tribologică a sistemelor de frânare ale autovehiculelor

Studies and research on the tribological behavior of vehicle breaking systems

Scientific coordinator:
Prof. univ. dr. ing. Filip Ilie

Author:
Eng. Andreea Cătălina Cristescu

Bucharest, 2023

CONTENTS **Thesis/Abstract**

FOREWORD

As I look back on the years spent in crafting this thesis, I recognize that I could not have reached this point without the support and contributions of many individuals who have influenced both my academic and personal journey.

First and foremost, I would like to express my heartfelt thanks and appreciation to my academic advisor, Prof. Dr. Eng. Filip ILIE, who deserves all my admiration and gratitude. He was not just an academic guide, but a mentor in the truest sense of the word. He provided insights and encouragement when it was needed. Through meticulous analysis, he shaped my outlook and helped me grow every day. His vision, patience, and passion for the field have been an inexhaustible source of inspiration for me. He guided me through challenges and taught me the value of perseverance in research.

I am also deeply grateful to the members of the Guidance Committee, Assoc. Prof. Dr. Eng. George Ipate, Prof. Dr. Eng. Gheorghe Voicu, and Prof. Dr. Eng. Ladislav David, who provided invaluable suggestions, methodological guidance, rigorous technical expertise, and encouragement during moments of doubt, playing a fundamental role in shaping and enhancing my research. I am indebted to them for this.

Special appreciation is dedicated to the Faculty of Biotechnical Systems Engineering and the Polytechnic University of Bucharest, who provided not only an excellent academic framework but also a community where I grew and learned.

I wish to thank the National Institute of Agricultural Machines in Bucharest – INMA, whose expertise and support in conducting experiments were essential to my research.

Throughout this journey, my parents, Otilia Cristescu and Florea Cristescu, have been my rock. I thank them for teaching me what determination means, for the long nights of discussions, and for the moments of quiet where their presence was all I needed. Every sacrifice, every word of encouragement, and every gesture of appreciation gave me the strength to continue, even when obstacles seemed insurmountable. It's impossible for me to express in words how thankful I am for everything they've given me.

Bucharest, 2023 **Eng. Andreea Cătălina CRISTESCU**

Chapter 1. IMPORTANCE OF THE TOPIC. OBJECTIVES OF THE DOCTORAL THESIS

1.1. Importance of the topic

In an era where the automotive industry is evolving at an impressive pace, the approach of studying the tribological behavior of the braking system under real traffic conditions provides an innovative and necessary perspective.

An essential aspect of this novel approach lies in the fact that many manufacturers do not focus enough on the study of real wear in everyday traffic scenarios. This research stands out by addressing this very gap, exploring how vital components of the braking system respond in variable traffic environments.

One of the critical components of today's vehicles is the braking system. As traffic becomes denser and the pace of urban life more hectic, brakes are used more frequently. Therefore, it is vital to understand how intensive use affects the tribological behavior of brake pads.

Tribological behavior refers to the study of the interaction between moving surfaces. In the case of brake pads, this study focuses on how different materials wear and interact under repetitive pressure and friction.

In heavy traffic conditions, constant and repeated braking can lead to rapid wear of the pads. Each brake application causes minor wear, which cumulatively can have a significant effect on the performance and lifespan of the pads, and more broadly, the braking system itself. Also, constant friction between the brake pad and disc can lead to microstructural changes, impacting the material's tribological properties.

Moderate traffic, though seemingly less demanding, also presents challenges. Without constant use, brake pads can be exposed to varying humidity conditions and road contaminants, which can influence the friction coefficient and, in turn, braking performance.

This doctoral thesis incorporates theoretical and experimental information from various fields: tribology, mechanics, mathematics, statistics, and computer science. This correlates with the establishment and development of the theoretical and experimental program and aligns with the thesis objectives.

By studying tribological behavior under these conditions, engineers can identify and develop more wear-resistant materials that maintain consistent performance over time, regardless of traffic intensity. This kind of study represents an innovative approach, focusing on the immediate and real aspects of urban life.

By adapting to these specific conditions, the automotive industry can develop safer vehicles, capable of delivering consistent efficiency and an extended lifespan of components. Moreover, as cities become more congested, anticipating and adapting to these changes become vital.

Consequently, studying the tribological behavior of brake pads in heavy and moderate traffic is not only innovative but also crucial for the future of urban mobility.

1.2. Objectives of the doctoral thesis

Braking systems are crucial for the efficient and safe operation of modern vehicles. A deep understanding of their tribological behavior under different traffic conditions is not just academic, but essential for the development of future technologies. The following parameters are the key objectives of this study:

Evolution of brake system wear - considering the variation in traffic conditions, it is essential to monitor and analyze how the components of the braking system wear out. This includes the evolution and degree of wear depending on the braking cycles and external conditions.

Friction coefficient - a vital factor for braking performance, the friction coefficient between the disc and brake pad can vary depending on traffic conditions and wear. Understanding this variation aids in optimizing the materials used and the design of components.

Braking force - monitoring and analyzing the force applied in different traffic scenarios allows us to understand the specific needs of each context/situation. This, in turn, influences the design of the braking system and its optimal operating capacities.

Wear coefficient - wear is inevitable, but its rate and type can vary. Determining the wear coefficient based on traffic intensity and other external conditions contributes to anticipating the lifespan of the braking system components and developing solutions to extend it.

Metallographic and chemical analysis - identifying the microscopic structure of the materials of the disc-brake pad pair, with a focus on phase distribution, grain size, and any defects or discontinuities. Moreover, there was an emphasis on determining the chemical composition of the materials used in braking components, highlighting the presence and distribution of key elements.

Efficiency of the braking system - ultimately, all these aspects contribute to the overall efficiency of the braking system. By analyzing brake performance under varying traffic conditions, possible weak points can be identified, and solutions can be developed to improve efficiency and vehicle safety.

Finite Element Analysis (FEA) method: - development of an FEA model for the braking system, taking into account the geometry, material properties, and boundary conditions. The behavior of the braking system during operation was simulated, identifying areas with high demands and potential critical points.

Modal/structural analysis - identifying the natural vibration modes and associated frequencies for the braking system, which can influence braking performance and the structural integrity of the components.

Correlating analytical data with experimental data - conducting practical tests to evaluate the braking efficiency of the system under different operating conditions. A comparison and validation of the results obtained through modeling with the experimental results were made, thus providing a complete picture of the system's real behavior.

Therefore, the objectives of this thesis focus on understanding and analyzing the operation of the braking system in real traffic conditions, by establishing its efficiency analytically and experimentally, based on the distance and braking/stop time, depending on the mass, vehicle speed, and the number of kilometers traveled.

The results and solutions will have significant implications for the automotive industry, leading to the development of safer and more reliable vehicles, by providing a solid foundation for optimizing braking systems, recommendations for designing and maintaining them in current conditions.

Chapter 2. THE CURRENT STATE OF RESEARCH ON THE TRIBOLOGICAL PROCESSES IN CAR BRAKING SYSTEMS

2.1. General Concepts

The necessity for a robust braking system increased with the advent of automobiles to provide superior performance, reliability, and safety. Thus, complex and sophisticated systems, such as the anti-lock braking system (ABS), ensure wheel contact with the driving surface. The electronic stability control system (ESP) monitors stability and detects skidding, and traction control systems ensure the vehicle's stability under various conditions [3, 4]. Consequently, the braking system must fulfill several critical and regulated requirements, such as:

- Safely stopping the vehicle;
- Immobilizing the vehicle on slopes;
- Ensuring the required deceleration;
- Providing progressive braking;
- Minimal effort on the driver's part;
- Proportionality between the effort applied to the braking system mechanism and the vehicle's deceleration;
- Application of braking force on both axles of the vehicle;
- Ensuring braking only occurs at the driver's intervention;
- Ensuring heat dissipation [1 - 4].

2.2. Components of the disc brake system with pads

The braking system is a set of parts that help the driver reduce the car's speed until it stops. Regardless of the vehicle's load and speed, it must operate on all wheels. It can function via a hydraulic, pneumatic, or hydropneumatic system.

Current regulations mandate the use of a dual braking system, structured in five different brake system configurations (Fig. 2.1):

- Parallel structure (II): the first circuit brakes the front axle, while the other circuit brakes the rear axle; this distributes the braking force on both axles.

- X structure: the first circuit brakes the front right wheel and the rear left wheel, while the second circuit brakes the front left wheel and the rear right wheel, distributing braking force diagonally.

- HI structure: the first circuit acts on both the front and rear axles, while a second circuit brakes simultaneously with the front axle.

- LL structure: the first circuit acts on the front axle and one rear wheel, while the second circuit acts on the front axle.

- HH structure: both circuits act on all four wheels of the vehicle simultaneously, making the braking system the most complex [3].

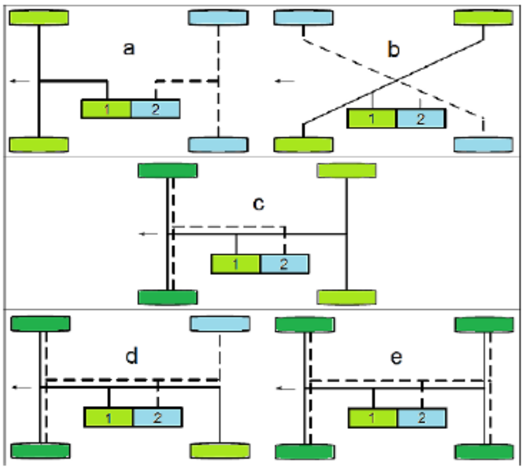

Fig. 2.1 Brake system configurations:
a- II structure, b- X structure, c- HI structure, d- LL structure, e- HH structure
1- first braking circuit, 2- second braking circuit. [3]

2.2.1 General overview of the Braking System

Disc brake systems with pads and drum brake systems are the two types used. Currently, drum brake systems are used on the rear axle of the car, but the disc brake system with pads is set to replace them [4].

Figure 2.2 shows a traditional braking system that does not require electrical assistance.

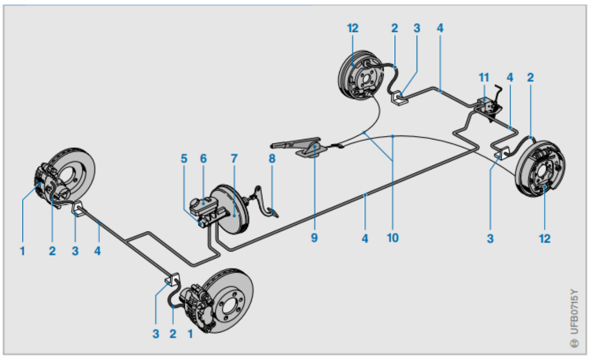

Fig. 2.2 Conventional braking system, on both axles of the car [4]: 1 - disc brakes, 2- brake hoses, 3 - brackets, 4 - main brake lines, 5 - master cylinder, 6 - brake fluid reservoir, 7 - servo motor piston, 8 - brake pedal, 9 - parking brake lever, 10 - handbrake cable, 11 - pressure regulating valve, 12 - drum brakes.

2.2.1. Component elements of disc brakes and pads

A braking system is necessary to stop or modify the speed of a vehicle depending on traffic and road conditions. Braking systems primarily utilize the vehicle's kinetic energy. A portion of the kinetic energy is transformed during a braking operation, but another part might be dissipated as vibrations in the case of frictional braking.

In disc braking systems, the brake pads are pressed against a rotating disc while braking. This generates heat due to the friction between the pads and the disc. This heat is then transferred to the external environment, thereby cooling the disc [6]. Disc braking systems have a caliper that is attached to the knuckle via bolts, a disc that is positioned between the hub and the wheel, and brake pads that are housed within the caliper. Hydraulic cylinders cause the disc to be clamped, stopping its rotational movement. Such a braking system is depicted in Fig. 2.3..

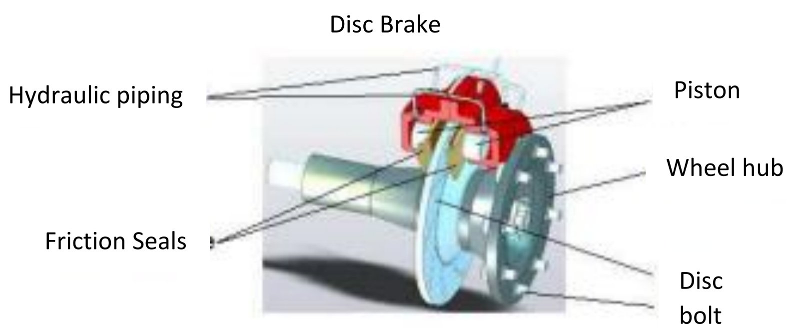

Fig. 2.3 Disc brake system[3]

2.3. Materials of the disc brake system with pads

2.3.1. brake disc materials

a) <u>Gray iron brake disc</u>

Gray iron is preferred for mass-produced automobiles because of its good cost-benefit ratio. Various types of alloys, such as nickel, iron-chromium, iron-manganese, iron-silicon, and others, are used as additives in the composition of the cast iron. Table 2.2 provides a relevant example for the production of brake discs by General Motors in Brazil, where gray cast irons are used with or without other chemical elements. [7].

b) <u>Ceramic brake disc</u>

Carbon fiber-reinforced ceramic matrix composites (CMC) with a carbon-silicon matrix are another option for brake discs, as they have better tribological characteristics than gray iron. Their main features include:

- low density;
- a high coefficient of thermal expansion compared to cast iron;
- constant friction coefficients and stability.

2.3.2. Materialele plăcuțelor de frână

The chemical, mechanical, and physical properties of the created friction materials can be modified by changing the mass percentage or types of elements in the composition. Initially, researchers concluded that the mechanical and physical properties of friction materials and wear properties are not directly related. As a result, every new formulation created must be tested to assess its wear and friction properties. This is done to ensure that the material created for the brake pad meets the minimum usage requirements. These tests include both on-road braking performance testing and abrasion testing. The construction of brake pads is shown in Fig. 2.4.

Fig. 2.4 Brake pad construction [3]
1- friction material; 2- heat resistant material; 3- adhesive layer; 4- metal plate; 5- damper.

2.4. Decommissioning of the disc brake system with pads

2.4.1. Decommissioning of the brake disc

The tribological behavior of cast iron is influenced by several parameters, such as the chemical elements that make up the brittle alloy and their morphology. There are several studies examining how different alloying elements affect the wear resistance of gray iron. It is known that silicon, chromium, and manganese improve the wear resistance of the brake disc [10].

<u>Brake disc lifespan</u>

Because there are many factors that affect the lifespan of a brake disc, figures show that some disc models last 10 to 15 times longer than others. While some discs can run 300,000 km, others only reach 20,000 km [12]. Thus, Fig. 2.5 shows various types of brake disc failures.

(a) (b) (c)

Fig. 2.5 Brake disc failures: (a) - cracks in the brake disc chamber; (b) - failure caused by refurbishment; (c) - variations in the thickness of the friction area [12]

2.4.2. Decommissioning of the brake pads

Apart from normal wear caused by overuse of the pads, there are several other circumstances that can damage brake pads. These include thermal degradation, tearing of the friction material, faulty installation, manufacturing defects, wear-related damages, and those caused by weather conditions (Fig. 2.6).

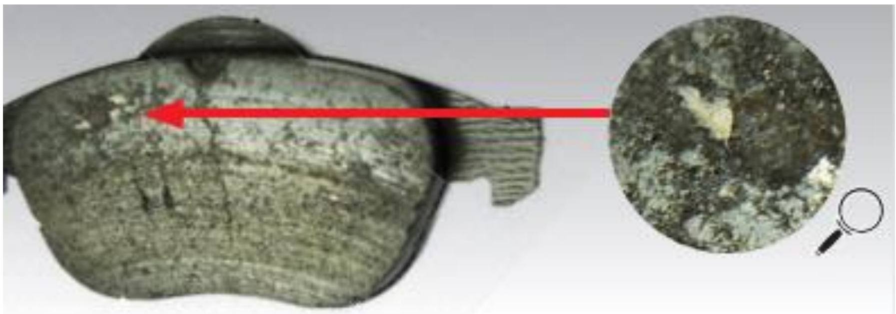

Fig. 2.6 Intrusion of metal shavings on the brake pad surface [12]

2.4.3. Operating Phenomena (thermal, dynamic, stick-slip)

The braking performance is influenced by the thermal and mechanical properties of the friction disc materials, the topography of the contact surfaces, as well as the body that forms as a result of wear processes [13, 14]. Therefore, to fully understand the behavior of brakes, it is essential to comprehend the changes that occur at the contact interface.

Thermal Phenomena

Studies on braking systems [17 – 19] have shown that the loading temperature increases the wear rate. The wear rate of a friction material with phenolic resin as a binder increases slowly below a critical temperature; however, if the temperature exceeds this limit, the wear rate increases rapidly, as shown schematically in Fig. 2.7..

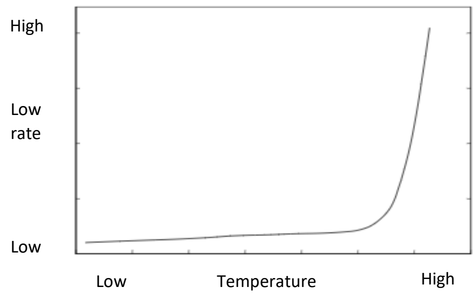

Fig. 2.7 Schematic Representation of Wear Dependency on Temperature [6]

Dynamic Loadings During Braking

The torque created by the wheel brakes reacts on the circumference of the tire where it contacts the ground when the brakes are activated. The magnitude of the frictional force in the case of brake locking directly depends on the torque generated by the wheel braking. Fig. 2.8 shows the forces affecting a two-axle vehicle decelerating on a horizontal roadway.

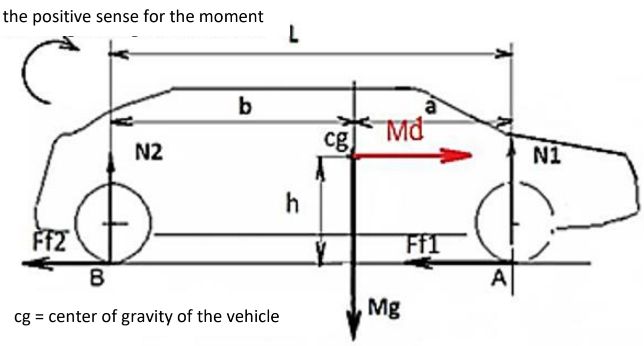

Fig. 2.8 Forces Acting During Vehicle Deceleration [3]

$F_{f1}+F_{f2}= F_{ft} = M\cdot d,$ (2.1)

where: F_{f1}, F_{f2} – the frictional forces of the front wheels (F_{f1}, (N)) and rear wheels (F_{f2}, (N)); F_{ft} – total frictional force, (N); M – vehicle mass, (kg) și d - vehicle deceleration, (m/s^2). $d= F_{ft}/M$. (2.2)

$N_1+N_2 = M\cdot g,$ (2.3)

unde: N_1, N_2 – the normal forces (reactions) on the front wheels, static (N_1, (N)) and rear wheels, static (N_2, (N)); $g = 9{,}81$ m/s^2 – gravitational acceleration.

Fenomenul stick-slip

One of the noises and vibrations that occur when a vehicle brakes is the stick-slip phenomenon. A series of intermittences in the braking process that are caused by the differences between the kinetic COF (μ_k) and the static COF (μ_s) are known as the stick-slip phenomenon. The static COF (μ_s) between the two contact surfaces of the brake disc and the brake pad must be greater than the kinetic COF (μ_k) for the sliding phenomenon to occur. Figure 2.9 shows the variation of COF (μ) over time (t) for the sliding phenomenon, where μ_{smax} is the maximum static friction [24].

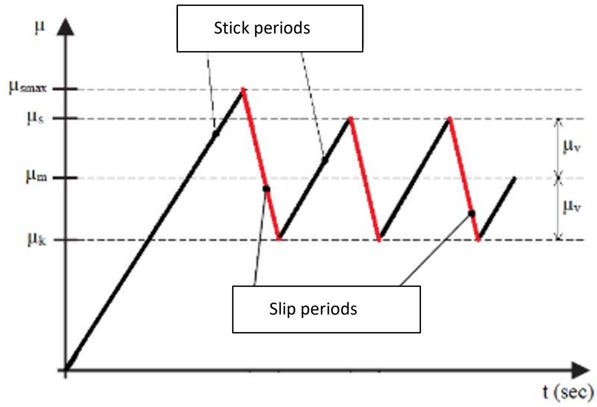

Fig. 2.9 Variation of the friction coefficient over time [24] (μ_m – average COF; μ_v – amplitude of the friction coefficients)

The stiffness characteristics of the brake system, the relative speed between the brake disc and the brake pad, and the local contact state between the friction surfaces influence the amplitude of the sliding phenomenon [24].

Conclusions

Given that the disc and pad brake is a complex system, expertise in various disciplines, such as tribology, material science, fluid dynamics, and vibrations, is essential.

Over decades of research and development, disc and pad brakes have evolved. Many phenomena are still not fully understood. Further development of non-linear finite element analysis (FEA) is crucial for a complete and realistic analysis of disc and pad brake systems. This could simulate the actual evolution of the contact interface.

Phenomena in the braking system, such as squeaking, vibrations, and judders, have drawn the attention of the research community. Due to the ongoing development of disc and pad brake systems, these have become increasingly rare; however, the problem has not yet completely disappeared. For the brake research community, the challenge of predicting brake actuation sensitivity remains.

Thus, studying the disc and pad brake system is critically important in the field of engineering and road safety. This advanced braking system offers numerous advantages over traditional technologies, such as superior braking power, efficient heat dissipation, and fade resistance. However, to optimally benefit from this system's performance, it's imperative to deeply understand its operating principles, component interactions, and factors that may influence its performance, like wear, temperature, material composition, and others. By carefully studying these aspects, engineers can develop innovative solutions for the continuous improvement of the performance of the disc and pad brake system, thereby enhancing road safety and offering drivers a more reliable and safer driving experience..

Chapter 3. STUDIES AND RESEARCH ON IMPROVING THE TRIBOLOGICAL PERFORMANCE OF AUTOMOBILE BRAKING SYSTEMS

3.1. Introduction

The primary objective of studying the braking system is to enhance its performance, considering the current situation and the advanced technological level that braking systems have reached, which ensures safe and stable braking even at high speeds. Adding ferrite magnets to the disc braking system increases the stopping power of the vehicle and represents an improvement in the braking system, as both the braking distance and time are significantly reduced. This braking system is mainly used on high-speed cars or motorcycles to ensure safe and stable braking [25].

3.2. Studies and research on improving the tribological performance of vehicle braking systems

Since braking is an essential process, the system components need to be carefully designed, manufactured, maintained, and monitored. To avoid repeating problems with the previous structures of braking systems, the research and development of new braking systems should be based on the experience of previous systems by testing their features that did not meet the requirements and the system's reliability itself. Therefore, the development of new systems should rely on the experience of previous systems to achieve high quality and reliability [27].

The primary purpose of braking mechanisms is to achieve the required braking torque to slow down the wheels and, ultimately, to stop. So, the reliability of the braking torque of any other technical system to fulfill the specified tasks without interruptions or defects is known as reliability [27].

Hence, to enhance the performance and reliability of braking systems, a series of studies and research have been conducted and are presented below.

3.3. Materials and research methods for the tribological performance of the disc and pad braking system

3.3.1 Overview

Disc and pad brakes operate to decelerate a vehicle by dissipating kinetic energy and through sliding contact between the friction material of the pads and the brake discs or rotors/discs that move along with the wheels. Figure 3.1 shows an example of a common assembly of the braking system. The sliding between pads and discs occurs at about half the vehicle's speed, and the pads usually cover between 10 and 15% of the area they describe on the disc [53].

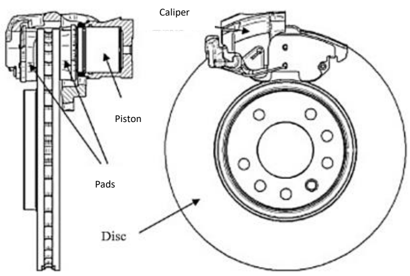

Fig. 3.1 Ventilated disc brake assembly with single-piston mobile caliper. [53]

3.3.2 Materials used in disc and pad braking systems

It's important to note that the friction of the friction pair is only half of the friction material. For many years, cast iron or steel discs or drums have been used in vehicle brakes, and most car friction materials have used cast iron as the contact surface.

Figure 3.2 shows the evolution of friction materials and the main issues they have faced in the last two decades, along with their solutions.

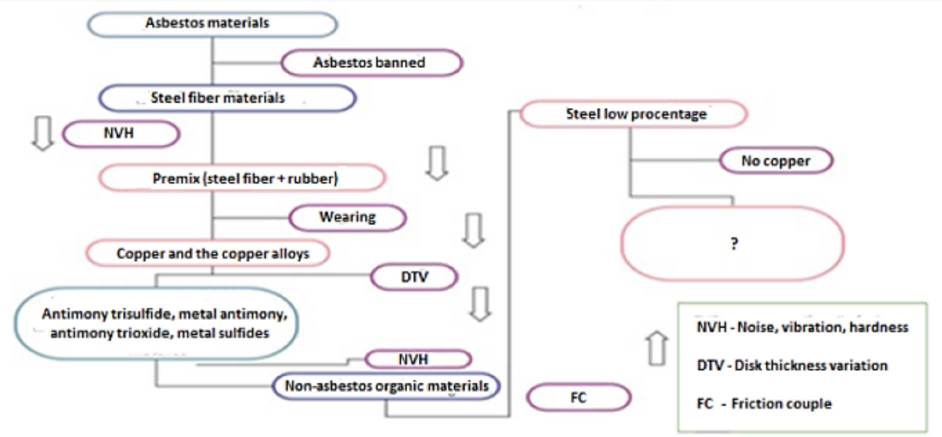

Fig. 3.2 - Evolution of friction material formulas in the last two decades [32, 55]

3.3.3 Methods for investigating tribological performance

Pin-on-Disc Tribometer (POD)

Table 3.9 contains a summary of the nominal contact pressures and sliding speeds used for testing. All tests are carried out for two hours to ensure that the condition is stable. Furthermore, Table 3.9 shows the CDF value, which corresponds to the value found when a steady state is achieved. Using the weights, the normal force (F_N) is applied and, implicitly, the nominal contact pressure. Then, the normal force, FN, is divided by the contact area of the pin with the disc to determine COF, μ_{POD}.

Finite Element Analysis (FEA)

The Abaqus software was used to perform the finite element analysis [62]. Fig. 3.3 displays a model of the components, while Fig 3.4 represents the discretized network of the braking system. For the caliper, a parabolic tetrahedral mesh was used, while hexahedral structures were employed for all other parts. The elements have an average size of 4 mm. A zero displacement constraint was established near the mounting points of the disc. The caliper's conduit wall and the back of the piston are subjected to system pressure, psys, and the disc is rotated [60].

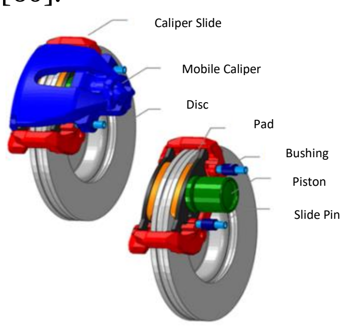

Fig. 3.3 Disc brake pad system [60]

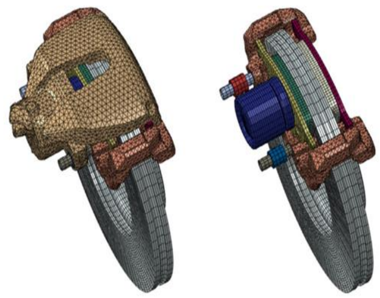

Fig. 3.4 Discretized mesh of the Breaking system [60]

3.4. Studies and research on improving friction materials

3.4.1 Influence of Temperature on Friction Materials

Thermal degradation of the friction material is one of the numerous reactions that can occur. Therefore, the COF (μ) changes with temperature. Generally, the COF (μ) increases slightly until the temperature of the disc or drum reaches around 200-250 °C, then decreases, as shown in Figure 3.5 (for composite/cast iron pair bonded with a resin binder), and Table 3.1 shows how the material characteristics determine the precise temperature variation.

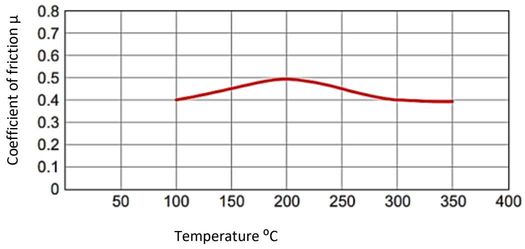

Fig. 3.5. Variation of the coefficient of friction, μ, for the composite/cast iron pair bonded with resin [32, 54]

Tablel 3.1 Example of specifications for friction material characteristics [54]

Design data (average values)	
Maximum tensile strength	15 MN/m^2
Maximum shear strength	25 MN/m^2
Rockwell hardness	25 MN/m^2
Density	1950 kg/m^3
Recommended maximum operating temperatures	
Continuous	250°C
Intermittent	350°C

3.4.2 Main characteristics of research methods

The aim of the research is to provide a simulation strategy to investigate the braking system's friction process as well as the performance of the friction material in question. These can be useful during the design phase of a new brake when there is no prototype available, and a specific friction material must be chosen to meet the system requirements and friction performance. Additionally, hard-to-study phenomena can be investigated using experimental tests, such as increasing COF during stops and increasing semi-local contact temperature.

3.4.3 Existing tribological performance research facilities

There are many different ways to test braking performance. Road testing and stand testing are the two types. The former should be done outdoors, and the latter can be done indoors. People using both detection methods require quite different conditions. Detection results of a parameter may differ when a car is tested with both methods [64].

A. Road testing method

The method is so simple and straightforward that anyone can see the dynamic change in braking performance while the testing tool/device is being driven directly. There are a number of factors, including human factors, road conditions, weather, temperature, and humidity, that can affect the results of road testing methods [64]. Figure 3.5 shows a model of a braking system testing equipment.

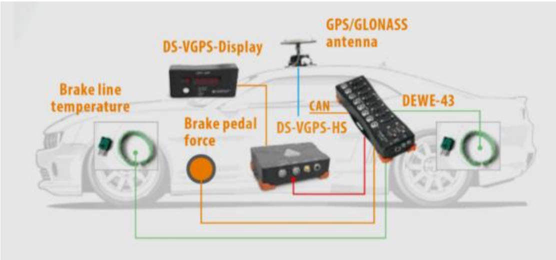

Fig. 3.6. Brake system testing equipment [65]

<u>B. Indoor testing method</u>

The testing process requires high speed and reliability. The indoor road testing method is used when questions arise about the measured data [64] and is performed on a test stand with independent engines to drive the rollers (Fig. 3.7). Additionally, it includes safety systems that detect the presence of the vehicle during the test and detect wheel slip during measurement. Each wheel has its own parameters [66].

Fig. 3.7 Brake system testing stand [66]

C. Experimental testing

a) <u>Tribometer</u>

The tribometer, also known as a tribotester, is an instrument used to replicate wear and friction at the interface between surfaces in relative motion under controlled conditions. Figure 3.8 schematically shows how the pin-on-disc, or roller-on-disc, is configured [67].

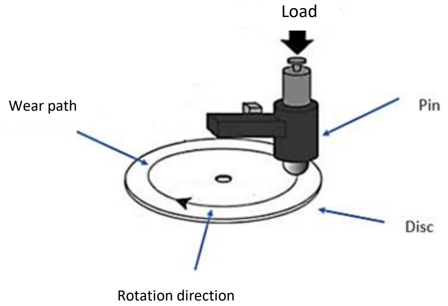

Fig. 3.8 Pin-on-disc tribometer [67]

3.5. Theoretical, experimental, and discussion of results

The piston-actuated pad exerts higher pressure on the inner part of the disc. The outer part of the smaller radius and the inner part of the larger radius have a transverse gradient as a result (Fig. 3.9 a and b). It is not very affected by disc slip as a direction because the ring pad has a contact pressure distribution with a gradient from small to large radii (Fig. 3.9 a and b). Figures 3.9 c and d show the slip rate. The slip rate is primarily affected by the disc's rotational speed, as shown in the image, and is higher in all analyzed distributions for larger radii. [60].

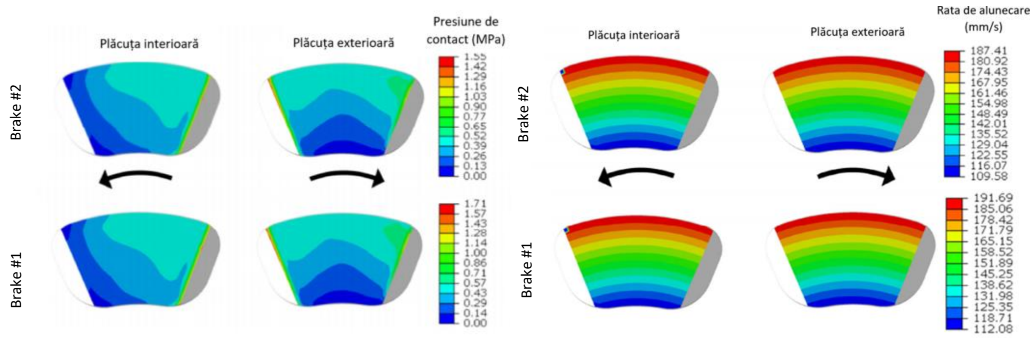

a) b) c) d)

Fig. 3.9 Contact pressure distribution for brakes #1 and #2 [60]: a) at the end of the braking process in one rotation direction; b) in the opposite rotation direction; c) slip rate during braking in one rotation direction; d) in the opposite rotation direction.
The arrows indicate the direction of disc rotation.

Conclusions

The simulation method was based on FEA and utilizes the global COFs (Coefficient of Friction) of a braking system as a function of contact pressure and sliding velocity. The following conclusions can be drawn by analyzing brake events in an urban traffic cycle and comparing the simulation to experimental results:

There is no significant difference in the COF created by the piston and the side plates of the rods for the studied braking system and brake events.

Regarding braking behavior, the experimental and simulated results align similarly, but the simulation exhibits a positive COF gap compared to the experimental ones.

The experimental and simulated results did not indicate a decrease in COF. This could be attributed to low-power braking, which allows neglecting thermal effects. Further studies with different braking systems are needed to fully validate the model, and other friction materials can be tested to generate a database with friction pv (pressure-velocity) maps.

Friction materials are crucial for both automotive brakes and other vehicles. Brake system designers need to have an understanding of friction and wear behavior characteristics, as well as the reasons why these characteristics differ.

Mechanical properties, friction, wear characteristics, and indications of temperature effects and recommended operating conditions are specified in commercially available friction materials. The COF of these materials varies depending on their composition, and vehicle manufacturers can choose friction materials based on their requirements; for example, passenger cars can use friction materials with a nominal COF value in the range of $0.38 < \mu < 0.45$, while commercial vehicles use a narrower nominal COF range, such as $0.35 < \mu < 0.40$. These provide a foundation for brake system design.

Although friction torque largely operates in accordance with the friction laws of Amontons, COF will change when the braking load increases, and the temperatures generated at the friction interface significantly rise.

Temperature changes lead to the most frequent COF variations. How much it changes depends on the friction material specification.

There is no other way to accurately determine the COF of a friction material than through testing.

Chapter 4. THEORETICAL AND EXPERIMENTAL ANALYSIS OF BRAKING PROCESS PARAMETERS UNDER HEAVY AND MODERATE TRAFFIC CONDITIONS

4.1. Introduction

The braking parameters of a car determine its safety and handling. The ability of a vehicle to decelerate rapidly and come to a complete stop in a short distance is referred to as braking. The kinetic energy of the vehicle is transformed into thermal energy in the braking mechanisms and in the contact area of the tires with the road surface when the vehicle is braking.

Mathematical models are frequently used to analyze the braking parameters of vehicles. However, in practice, the values of braking and deceleration parameters are random [75].

4.2 Analysis of braking process parameters under heavy and moderate traffic conditions

4.2.1. General Overview

By utilizing simulations based on finite element analysis, Kchaou and colleagues [77] analyzed changes in parameters such as the coefficient of friction (COF), temperature, and deformation. Although these types of studies provide conclusive values, they also have disadvantages. One of these disadvantages is the necessity of using simple assumptions in complex contexts [79].

The coefficient of adhesion, which varies depending on the type of road surface, indicates the tire's grip on the road surface. If the vehicle is traveling on a hard-surfaced road, soil resistance to shear is more important than friction. The movement of tires creates hydrodynamic pressure on water when moving on a wet, hard-surfaced road. Tires with shallow tread depth can cause hydroplaning when the tires lose contact with the road surface at high speeds [71].

4.2.1. Theoretical aspects of vehicle braking process parameters

Displacement and Braking Effort

The value of kinetic energy produced by a moving vehicle varies depending on its mass and speed. This energy is supplied by the engine to accelerate the vehicle from rest to a certain speed. However, when the vehicle is slowed down or brought to a stop, this energy is partially or completely dissipated. Therefore, the function of the brake is to continuously convert the kinetic energy of the vehicle into thermal energy through friction (Figure 4.1) [52].

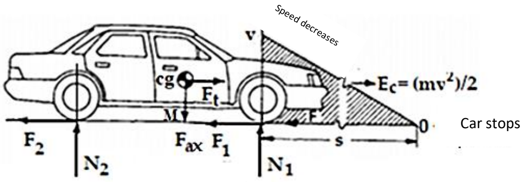

Fig. 4.1 Braking conditions of the vehicle [88]

Braking distance and efficiency

Braking distance is one of the important parameters for determining the efficiency of the braking system, η. Thus, the braking efficiency, η, of a vehicle is defined as the braking force, F, generated as a percentage of the total weight force (or the total mass), M, of the vehicle

[52], or the coefficient of friction, η, is the ratio of the braking force, F, to the weight of the vehicle, expressed as a percentage [94], through the relationship:

$$\text{Braking efficiency } (\eta, \%) = \frac{Braking\ force,\ F}{Vehicle\ mass,\ M} \times 100 \tag{4.1}$$

Considering that the mechanical work, W = F·S, done by the vehicle's braking system from the moment of braking until the complete stop of motion (the final velocity of the vehicle will be zero, v = 0) must be equal to the initial kinetic energy of the vehicle, E_k, the equation/relationship (4.1) is obtained in the form::

$$\text{Braking efficiency } (\eta,\%) = \frac{The\ square\ of\ the\ initial\ braking\ speed\ (v,\ m/s)}{2 \times gravitational\ acceleration\ (g,\ m/s^2) \times braking\ distance\ (S,\ m)} = \frac{v^2}{2gS} \times 100, \tag{4.2}$$

Similarly, the coefficient of friction (COF) is a measure of the ratio between the frictional force and the normal load between the frictional surfaces, expressed as:

$$\text{Coeficientul de frecare (COF), } \mu = \frac{Friction/Braking\ force\ ,\ F}{Normal\ load,\ N} \tag{4.3}$$

Thus, a braking efficiency (braking yield, η) of 100% is equivalent to a coefficient of friction (COF), μ = 1, meaning:

$$\eta(100\%) = \mu = F/N = 1. \tag{4.4}$$

4.2.2. Metode și principii de modelare a parametrilor de testare

Finite Element Analysis model

In this study, researchers employed a testing procedure to model a 3D axisymmetric segment of a ventilated gray cast iron EN-GJL-250 disc brake, which had 41 vanes (as shown in Fig. 4.2). Equipment related to material properties and the vehicle for the analytical calculation in this study is presented in Tables 4.7 and 4.8. During the braking operation, the ambient temperature was 30°C. As per Fig. 4.9, it was assumed that the thermal load was uniformly applied to the friction surface.

Table 4.1 contains information relevant to equation (4.4) and the values of vehicle and braking parameters. [106].

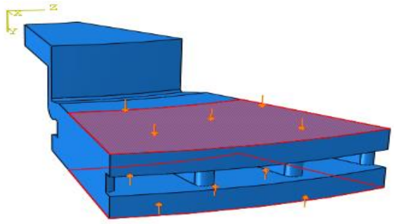

Fig. 4.2 3D CAD model of an axiometric segment from a ventilated disc brake with applied loads [106]

Table 4.1: Values of vehicle and braking parameters [106]

Nomenclature and Units	Value
Vehicle mass – M (kg)	1760
Initial velocity – v_0 (km/h)	100
Acceleration – a (m/s^2)	1.73
Deceleration - d (m/s^2)	9.8
Front/rear brake distribution – $d_{f/s}$ (%)	76
Outer friction radius of the pad – r_0 (mm)	139
Inner friction radius of the pad – r_i (mm)	93.5
Percentage of heat absorbed by the disc – η_{disc} (%)	99

4.3 Experimental analysis of brake process parameters under heavy and moderate traffic conditions

4.3.1 General Information

The operational limitations of small brakes are related to reducing vehicle weight with lightweight components. Although cast iron is heavy, it is the best traditional material for disc brake rotors. This is because it has high density, high conductivity, low thermal expansion, and a high maximum operating temperature (MOT) of over 600°C, which provides excellent volumetric thermal capacity.

Even though lightweight materials technologies are not suitable for maximum braking loads in frictional braking, they can be used for emergency braking at lower loads. For example, aluminum matrix composite brake discs (Al MMC) are lighter than cast iron but have reduced operational life at 400°C..

4.3.2. Analysis of experimental research methods used in brake process parameter analysis

Driving in an urban area or heavy traffic can consume a lot of braking energy, even at low to medium speeds. An electric motor/generator (M/G)-based regenerative braking system (RBS) with a 30 kW capacity, similar to the one found in the Toyota Prius, was modeled to demonstrate the energy involved and how it changes with speed and deceleration rate in typical city driving cycles.

The modeling used the ADVISOR software package, which predicts fuel consumption, performance, and emissions for six urban driving cycles: ECE, NEDC, INDIA, UDDS, and FTP. [84].

4.3.3 Potential applications of experimental research methods

The chassis dynamometer performs wheel torque measurements under various simulation conditions. A motor unit, as illustrated in Fig. 4.3, is included in it, along with the main electric power supply unit, a controller, a computer with analysis software, and real-time data logging wiring [109]. Standard driving cycles such as ECE/EG, US06, and FTP75 can be simulated using the dynamometer.

Fig. 4.3 The chassis dynamometer is attached to the front wheels of the car [84, 86] with the following specifications: maximum power output: 100 kW, which the vehicle can both generate and absorb; instantaneous maximum torque: 2500 Nm; continuous maximum torque: 1180 Nm; maximum hub speed: 2100 rpm, equivalent to the vehicle's maximum speed of 250 km/h.

4.3.4 Experimental testing methods used in brake process parameter research

Chassis Dynamometer

Chassis dynamometers are used to evaluate a variety of vehicles, from small cars to light trucks, at speeds of up to 250 km/h. The system can have one, two, or four rollers, with a motor that can drive each axle or each individual roller.

Fig. 4.4 *Chassis dynamometer* [114]

Testing Stand:

Figure 4.5 presents inertia dynamometers commonly used for testing [107].

Fig. 4.5 Inertia dynamometers are used for tests [107]

Conclusions

There are numerous studies that create models and simulate reality very well. However, the results need to be verified using experimental methods to validate real-world operational outcomes, or even through data sampling during operation.

Some studies focus on heating the discs and pads and heat dissipation. Further research examines the impact of thermal requirements on the durability and reliability of components. Many studies do not capture real-time data from operation.

The tribological properties (friction and wear) of braking systems/mechanisms used in motor vehicles, trailers, and other terrestrial means of transport are influenced by a variety of factors, including, but not limited to, the design of the braking mechanism/system, the materials used in its manufacturing, and the service conditions.

Since friction is a typical stochastic process with a number of random influences, it is almost impossible to predict the performance and reliability of such a type of mechanism/system theoretically or analytically. Evaluating the tribological properties of braking mechanisms/systems is a rather complicated task.

As a result, experimental techniques are widely used to assess the performance of brakes and clutches. This is especially applied to brakes and braking systems that need to be tested and approved in accordance with various regulations and safety requirements related to road safety.

Chapter 5. ESTABLISHING THE METHODOLOGY AND EQUIPMENT REQUIRED FOR EXPERIMENTING WITH THE BRAKING SYSTEM UNDER HEAVY AND MODERATE TRAFFIC CONDITIONS

5.1. Introduction

A motor dynamometer is not as sophisticated or large as a brake dynamometer. Brake dynamometers are capable of simulating the circumstances the braking system will encounter in a much shorter time frame. This means a dynamometer has the ability to model the mass, inertia, and performance of a vehicle. Additionally, a brake dynamometer can replicate road conditions by simply spinning the braking system. A large electric motor ranging from 75 to 200 horsepower is used for this purpose, and a computer controls the motor and can simulate various vehicle inputs. The motor simulates the kinetic energy of the moving vehicle by providing torque that sets the wheel in motion. In other words, it rotates the brake system at an interval of "n" rpm, which equals the desired speed [115].

5.2. Facilities used in brake system testing

5.2.1. Nussbaum VISIO Dynamometer

The Nussbaum VISIO dynamometer, version 2.0.1.4 STD, with a set of BT110/410 rollers (3.5 kW, 6.0 kN, 5.0 km/h), was used to measure the parameters of the brake system of the tested vehicle, as presented in Figure 5.1. [116]

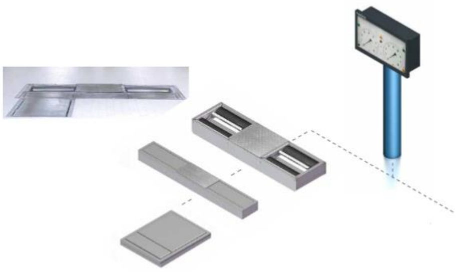

Fig. 5.1 5.1.1. Nussbaum VISIO Dynamometer [116]

5.2.2. Dynamometer Rollers

In the case of brake system efficiency testing, most countries use a test speed of 5 km/h, while loaded carriers usually use the maximum braking force range of 8 kN.

To determine the braking efficiency, the assistance of an optional weighing device mounted under the rollers or, in the case of a test belt, under the belt is required. Therefore, the test stand is equipped with such a device that measures the mass of the vehicle under test [116]. The technical data of the dynamometer rollers used in testing are presented in Table 5.1.

Table 5.1 Technical Data of BT 110/410 Rollers

Characteristic	Maximum Permissible Value
Permissible Axle Load (kg)	4
Measurement Range (kN)	6
Test Speed (km/h)	5
Roller Diameter (mm)	204
Roller Surface	Welded
Test Surface Width (mm)	800-2200
Motor Power (kW)	3.5
Roller Set Dimensions (mm)	2332 x 668 x 265
Control Panel Dimensions (mm)	582x500 x 210

5.3. Testing methodology and results on the test stand

5.3.1. Metallographic analysis of the brake disc and pads

Following the conducted research, it was found that there is a lack of specialized studies specifically tracking the wear trend of the braking system under conditions of both heavy and moderate traffic. The absence of a calculation methodology determining the wear trend of the braking system under intensive operating conditions, which could jeopardize traffic participants' safety, was observed.

Understanding the metallurgical and chemical structure of the materials used in the tested vehicle's disc and brake pads was considered of great importance. To achieve this, samples were taken from the disc and brake pad material.

Figure 5.2 depicts the metallographic structure of the brake disc material (magnified 500:1, from the selected area). Based on the chemical composition, it represents a pearlitic gray cast iron with: 3.34% C; 2.15% Si; 0.64% Mn; 0.03% P, 0.02% S; 0.04% Cr; 0.047% Cu; 0.041%, along with other chemical elements like Ni; Mo; Sn; V; Ti; W; Sb in very small quantities that cannot be detected, and the carbon equivalent (CE) is approximately ≈ 4.26.

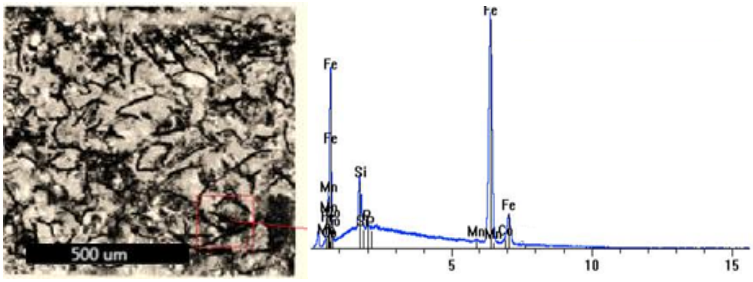

(a) (b)

Fig. 5.2 The metallographic structure of the brake disc material (a); the EDS spectrum of the delimited area (b)

The metallographic structure of the brake disc material (Fig. 5.2a) contains: pearlite (dark islands); secondary ledeburite (white dotted field); secondary cementite (white areas); fine lamellar graphite (dark lamellar islands), and in the EDS spectrum (Fig. 5.2b), you can see the chemical elements that make up the chemical composition of the pearlitic gray cast iron. Overall, the structure of the pearlitic gray cast iron appears normal and devoid of structural defects.

EDS analysis is an analytical technique that allows for the chemical characterization/elemental analysis of materials from the surface of the tested material.

The sample from the brake pad, based on its metallographic structure (magnified 500:1, from the selected area) and chemical composition, is a metal composite with: 10% C; 9% O; 1% Na; 5% Mg; 6% Al; 12% Si; 7% S; 2% K; 14% Ca; 6% Ba; 2% V; 5% Cr; 2% Mn; 19% Fe, as presented in Fig. 5.3.

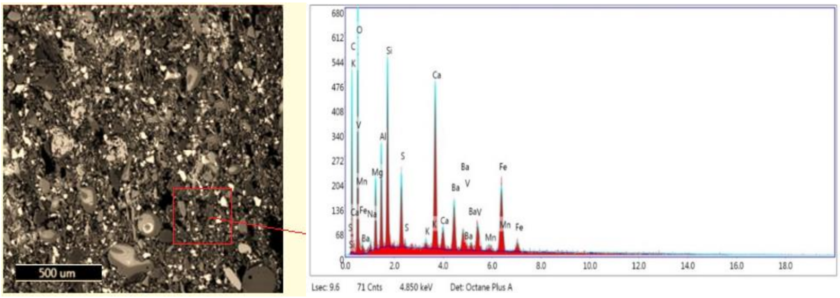

(a) (b)

Fig. 5.3 The metallographic structure of the brake pad material (a); the EDS spectrum of the delimited area (b)

Therefore, the metallographic structure of the brake pad material (Fig. 5.3a) contains a variety of metallic materials in significant proportions (totaling 51%), as well as carbon at 10% (making it a metal composite). In the EDS spectrum (Fig. 5.3b), you can observe the chemical elements that make up the chemical composition of this metal composite. Overall, the structure of the metal composite appears normal and devoid of structural defects.

Vehicle under test

The vehicle under test was subjected to conditions of heavy traffic in urban areas, where the braking system was heavily used, with frequent brake pedal activation. Additionally, the vehicle was used in extra-urban areas (moderate traffic) at constant speeds, where the braking system was not intensively utilized.

The vehicle is equipped with a disc brake system with brake pads on both the front and rear axles. On the front axle, the vehicle has ventilated discs (Fig. 5.4a), while solid discs are present on the rear axle (Fig. 5.4b).

a) b)

Fig. 5.4 Brake Disc: a) ventilated brake disc; b) solid/unventilated brake disc

5.3.2. Experimental Determination of Brake System Efficiency After Replacing Brake Pads (worn discs, new pads)

Following the installation of a new set of brake pads, the vehicle underwent a series of tests on the brake system testing stand. Along with the brake pad replacement, the brake fluid was also replaced to achieve the best possible brake system performance.

It is important to note that the brake discs showed signs of wear, such as scratches on the contact surface, as well as rust.

In Figure 5.5, the scratches on the surface of the brake disc are presented. These are the wear marks caused by the use of defective brake pads, which lead to brake disc damage. Figure 5.6 shows the degradation of the brake disc caused by rust presence..

Fig. 5.5 Scratches and wear marks present on the surface of the brake disc

Fig 5.6 Brake disc with rust marks

Following the removal of the brake pads, you can observe the degree of wear compared to a new set of brake pads, as well as signs of wear, including material separation. These aspects are presented in Figure 5.7.

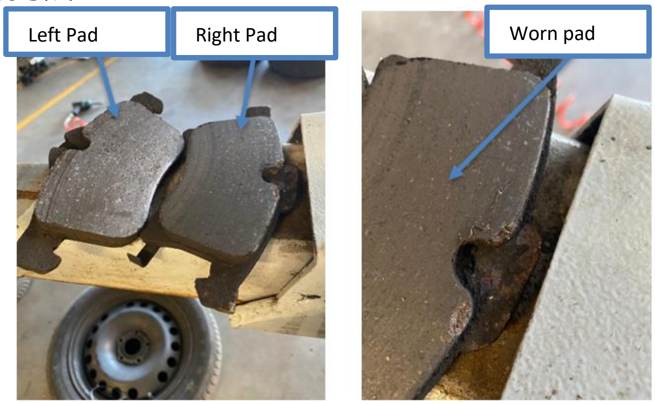

Fig 5.7 Wear level of brake pads

Following the replacement of the brake pads, a series of tests were conducted on the braking system to determine its efficiency, braking force, and other parameters related to the entire braking system.

The parameters of the braking system were determined at a speed of 5 km/h..

5.3.3. Experimental results obtained through brake force testing after brake pad replacement

Experimental results were obtained through tests on the brake force testing stand under various conditions of mass and kilometers traveled.

Centralized Results

Following the tests conducted on the braking system with the use of the brake dynamometer, key parameters of the braking system were determined, and their results are presented in a centralized manner in Table 5.2.

Table 5.2 Results Obtained from Service Brake and Parking Brake Testing

Parameter	Unit of measurement	Admissible limit	Measured value
Total service brake force	kN	-	9.14
Total parking brake force	kN	-	2.94
Service brake force difference	%	30	5
Service brake efficiency, relative to the total mass of the vehicle	%	50	73
Parking brake efficiency, relative to the total mass of the vehicle	%	16	23

5.3.4. Experimental determination of the efficiency of the worn disc and brake pad system

Following the completion of 18,664 km, the vehicle underwent a new set of tests, with a testing procedure similar to the one described earlier.

To track the wear trend of the braking system, the vehicle's discs and brake pads were not replaced. Thus, the vehicle with worn discs and brake pads underwent a series of tests to determine the performance and parameters of the worn braking system. The testing stand and the vehicle undergoing testing are presented in Figure 5.8 and Figure 5.9.

Fig 5.8 The brake system testing stand

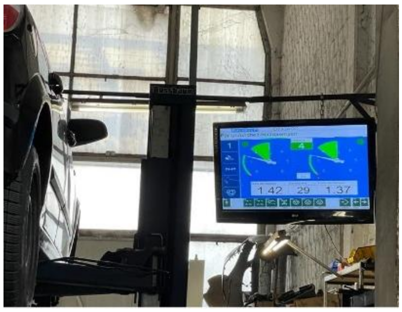

Fig 5.9 Display of measured brake system parameters: deceleration, braking forces, left/right wheel

The rollers of the Nussbaum VISIO brake dynamometer set the vehicle's wheels in motion at a speed of 5 km/h. With the help of the software, the test stand collects data related to brake system parameters, determined through successive brake activations. The operator performs these successive brakes, and then the test stand's software generates a report with accurate results..

5.3.5. Experimental results obtained through brake force testing on the test stand - case with worn discs and brake pads

Three test samples (I, II, and III) were considered based on mass and the number of kilometers traveled to determine the experimental results useful for determining the efficiency of the brake system of the tested vehicle. To compare the results, the vehicle's mass was modified for each sample, while the number of kilometers remained the same.

I. <u>Test 1</u>

The vehicle was placed on the rollers of the test stand, simulating a speed of 5 km/h. The brake was activated several times to obtain the most accurate results. Additionally, a sensor was attached to the brake pedal to measure the pedal's force, aiming to determine the difference in braking force.

The arrangement of the vehicle on the test stand for testing the front axle's service brake is shown in Figure 5.10.

(a) (b)

Fig. 5.10 Testing the front axle's brake system - Sample 1: (a) positioning the vehicle on the stand; (b) data collection method/signals and transmission to the database

Centralized Results - Test 1

Following the measurements, key parameters of the brake system were determined and are listed in Table 5.3

Table 5.3 Results obtained from the tests - Test 2

Parameter	Unit of measurement	Admissible limit	Measured value
Total service brake force	kN	-	9.05
Total parking brake force	kN	-	2.98
Service brake force difference	%	30	15
Service brake efficiency, relative to the total mass of the vehicle	%	50	63
Parking brake efficiency, relative to the total mass of the vehicle	%	16	20

II. <u>Test 2</u>

The testing methodology is similar to Sample 1, except that the vehicle's mass increased from 1462 kg to 1480 kg (by 18 kg), as follows:

To determine the brake system parameters as close to real values as possible, the vehicle was weighed.

Centralized Results - Test 2

Key brake system parameters were determined/measured following the tests and are presented in Table 5.4.

Table 5.4 Results obtained from the tests - Test 2

Parameter	Unit of measurement	Admissible limit	Measured value
Total service brake force	kN	-	10.06
Total parking brake force	kN	-	2.71
Service brake force difference	%	30	17
Service brake efficiency, relative to the total mass of the vehicle	%	50	69
Parking brake efficiency, relative to the total mass of the vehicle	%	16	18

III. <u>Test 3</u>

Following the same testing methodology as in the previous tests, test 3 was conducted, where the vehicle's mass increased from 1480 kg to 1524 kg (an increase of 44 kg) as follows: Similar to the previous tests, the vehicle was placed on the test stand, simulating a speed of 5 km/h.

Centralized results - Test 3

The experimental trials led to the determination of the brake system's efficiency, along with other key parameters. These are presented in Table 5.5.

Table 5.5 Results obtained from the tests - Test 3

Parameter	Unit of measurement	Admissible limit	Measured value
Total service brake force	kN	-	8.88
Total parking brake force	kN	-	2.91
Service brake force difference	%	30	5
Service brake efficiency, relative to the total mass of the vehicle	%	50	59
Parking brake efficiency, relative to the total mass of the vehicle	%	16	19

Table 5.6 presents the brake system parameters based on the vehicle's mass and the number of kilometers traveled on each axle..

Table 5.6 Parameters of the braking system according to the mass and mileage of the vehicle

		Vehicle mass 1480 kg- 115477 km		**Vehicle mass 1462 kg - 134141 km**		**Vehicle mass 1480 kg - 134141 km**		**Vehicle mass 1524 kg - 134141 km**	
Parameter	**Measurement Unit**	**Axle 1**	**Axle 2**	**Axle 1**	**Axle 2**	**Axle 1**	**Axle 2**	**Axle 1**	**Axle 2**
Braking force on the left wheel	kN	2.99	1.7	2.68	1.57	2.93	1.84	2.88	1.6
Braking force on the right wheel	kN	2.84	1.61	3.17	1.63	3.54	1.75	2.74	1.66
Braking force on the axle	kN	5.83	3.31	5.85	3.2	6.47	3.59	5.62	3.26
Difference between braking forces	%	5	5	15	4	17	5	5	4
Axle ratio	%	73	74	63	62	69	68	58	60

The axle ratio is defined as the ratio between the braking force (F_1 or F_2) and the vertical load on the axle (N_1 or N_2), usually expressed as a percentage, according to the following equations:

- for axle 1 (front axle), RPA_1, % = $(F_1/N_1) \times 100$, (5.1)
- for axle 2 (rear axle), RPA_2, % = $(F_2/N_2) \times 100$, (5.2)

Where: $F_{1,2}$ is converted from kN to kg, which means it is multiplied by the gravitational acceleration, $g = 9.81 \approx 10$ m/s^2 (rounded to 10 m/s^2, as commonly used).

So, considering the case of the vehicle with a mass, m = 1526 kg, with m_1 = 974 kg on axle 1 (front axle) and m_2 = 552 kg on axle 2 (rear axle - see Table 5.15 from thesis), then the braking force on axle 1 is F_1 = 5.62 kN, and F_2 = 3.26 kN on axle 2 (see Table 5.19 from thesis), we get:

- braking force in kg, $F_1 = 5.62 \times 100 = 562$ kg, $F_2 = 3.26 \times 100 = 326$ kg, respectively

RPA_1 = (5.62 kN / 974 kg) x 100 = (5.62 x 100 kg / 974 kg) x 100 = 57.70% ≈ 58%, and

RPA_2 = (3.26 kN / 552 kg) x 100 = (3.26 x 100 kg / 552 kg) x 100 = 59.06% ≈ 60%.

Therefore, the correlation between the measured values (see Table 5.19 from thesis) and the analytically calculated values is confirmed, with the note that they have been rounded up. The way the parameters from Table 5.6 vary with the mass and the number of kilometers traveled is shown in Figure 5.11.

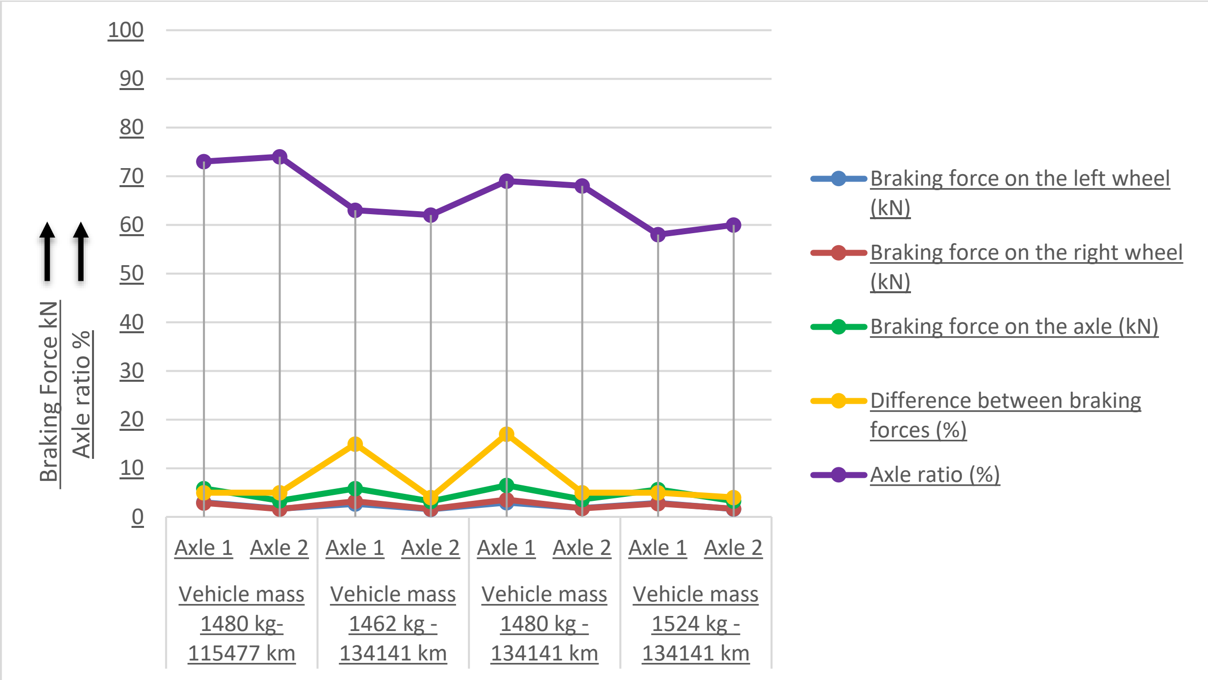

(a)

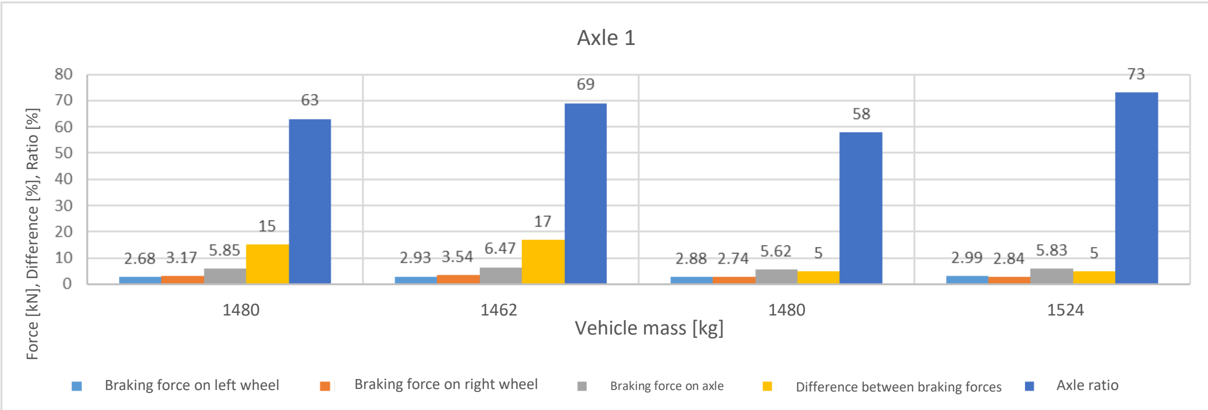

(b)

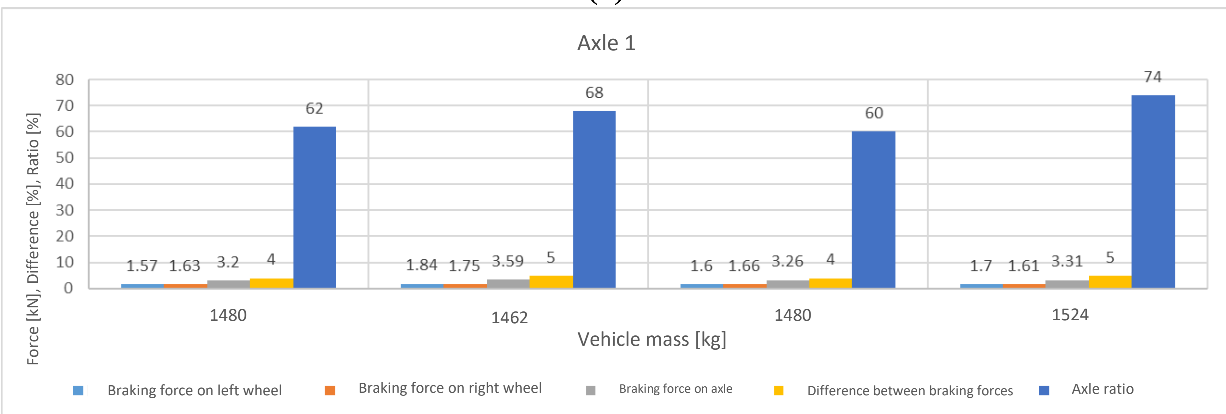

(c)

Fig. 5.11 Variation of braking system parameters as a function of mass (4 different mass values) and kilometers traveled (2 different distances, 115,477 and 134,141 km) of the vehicle: (a) graphical representation; (b) and (c) representation in a histogram.

Analysing Table 5.6 and Fig. 5.11, it can be observed that the braking forces on the wheels are very close, while the braking force on the axle is slightly higher, with each of them reaching a maximum at the tabulated mass values of 1480, 1462, 1484, and 1524 kg. On the other hand, the Axle Load Ratio (Raportul pe axă) has a relatively less contradictory trend compared to the difference between the braking forces, with maxima at a mass of 1480 kg and minima at masses of 1462 and 1524 kg. This could be explained by the fact that braking forces vary relative to traffic conditions (dry, wet road surface, gradient, even operator variations, etc.).

Next, both in tabular and graphical form, the evolution of the braking system's efficiency and the measured braking force in relation to the vehicle's mass and the number of kilometers traveled are presented in Table 5.7 and Fig. 5.11..

Table 5.7 – Braking System Efficiency Based on Vehicle Mass (4 Different Values) and Kilometers Driven (2 Different Values)

	Vehicle mass 1480 kg- 115477 km	**Vehicle mass 1462 kg - 134141 km**	**Vehicle mass 1480 kg - 134141 km**	**Vehicle mass 1524 kg - 134141 km**
Braking Difference of the Service Brake	5	15	17	5
Service Brake Efficiency Relative to Total Vehicle Mass	73	63	69	59
Parking Brake Efficiency Relative to Total Vehicle Mass	16	16	16	19

Braking efficiency refers to the ability of a vehicle's braking system to convert the vehicle's kinetic energy into heat (through friction), thereby slowing down or stopping the vehicle.

The formula for calculating braking efficiency is:

$$\eta = \frac{Total\ Applied\ Braking\ Force,\ F_t}{Maximum\ Possible\ Braking\ Force,\ G} \times 100\ \%, \qquad (5.3)$$

where: the applied braking force is the sum of the braking forces on each wheel of the vehicle
Using the data obtained on the brake testing stand (see Table 5.19 from thesis), we can calculate the braking system efficiency, η, as follows:

- efficiency of the service brake:

$F_t = F_1 + F_2$, (5.4)

It results in: F_t = 5,62 + 3,26 = 8,88 kN = 8.880 N, and G = m × g, (5.5)
where : m = 1524 kg, g = 9.81 ≈ 10 m/s^2 and we obtain G = 1524×10 = 15240 N .
In this case, the efficiency of the service brake is given by, $\eta_s\% = \frac{F_t}{G} \times 100 = \frac{8880}{14976.06} \times 100 \approx 59.3\%$ (58,26 ≈ 59 %)

- the efficiency of the parking brake:

F_t = 2.91 kN = 2910 N; G = 1524×10 = 15240 N , results

$\eta_p\% = \frac{F_t}{G} \times 100 = \frac{2910}{14976.06} \times 100 \approx 19.4\%$. (19,09 ≈ 20 %).

By comparing the analytically calculated braking efficiency values with the measured ones (see Table 5.7, for a vehicle mass of 1524 kg), we can see that the same value (59%) was obtained, with a small difference (1%, 20 instead of 19%), due to rounding up.

In Figure 5.12, you can observe the variation of the braking system efficiency as a function of vehicle mass (1480 kg, 1462 kg, 1480 kg, 1524 kg) and kilometers driven (115,477 km, 134,141 km) for the vehicle.

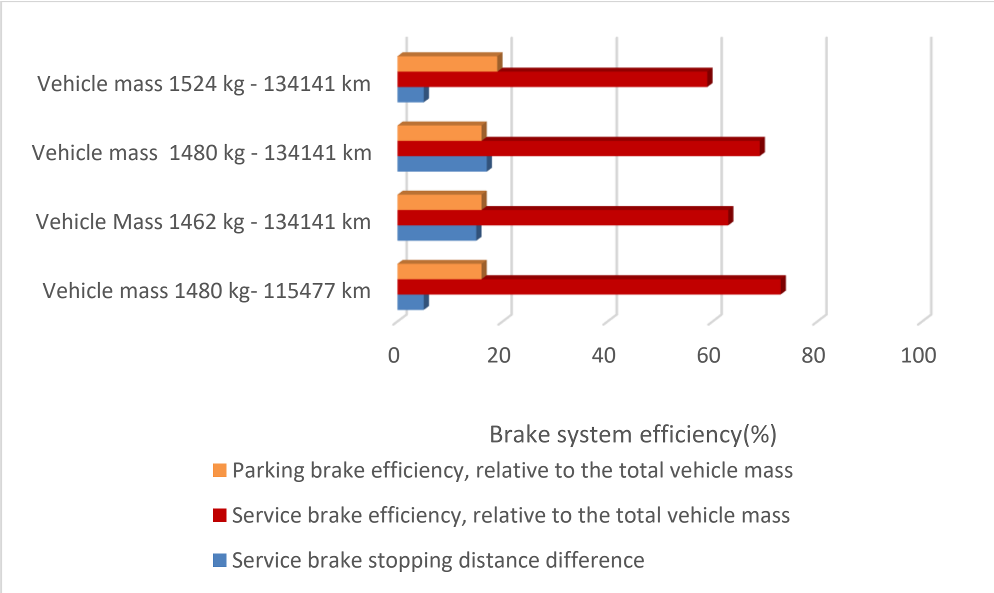

Fig. 5.12 he evolution of the braking system efficiency depending on the variation in vehicle mass (4 different values) and kilometers driven (2 different values) of the vehicle

Conclusions

There are many studies and research based on models that closely mimic reality, but studies with real-time operational data are still limited. The experimental results in this work have been validated through experimental testing methods that closely resemble operational reality.

The braking system of the tested vehicle was tested in accordance with the regulations and safety standards applicable to road safety.

Following the experimental tests, a significant reduction in the braking system's efficiency was observed after just 18,664 km of driving in both heavy and moderate traffic conditions.

Under normal vehicle loading conditions (a mass of 1524 kg), the braking system efficiency was observed to be only 59%. Considering that the minimum acceptable point for braking system efficiency is 50%, the results are concerning, suggesting the need to replace the braking system at a much shorter interval than normally recommended.

From the presented graphs, a significant reduction in the braking system efficiency, namely 14%, was observed in just 18,664 km of driving. The vehicle was used in urban traffic conditions, leading to accelerated wear of brake pads and discs.

At the same time, experimental tests have shown that recommendations regarding the frequency of replacing brake discs and pads do not conform to the actual braking system.

It is necessary to study the parameters of a new braking system in order to estimate its wear time. After field tests of the current braking system, it will be replaced. Tests on the stand and in the field will be conducted with the new braking system to determine its efficiency.

Chapter 6. EXPERIMENTAL RESULTS REGARDING THE TRIBOLOGICAL BEHAVIOR OF THE BRAKING SYSTEM

6.1 Introduction

In order to determine the tribological behavior of the braking system under heavy and moderate traffic conditions, several successive tests were conducted on a vehicle to monitor the wear trend of the brake pads, as well as the brake discs, and the evolution of the braking system's efficiency. To achieve this, tests were carried out on a dynamometer stand as well as in real traffic to determine the efficiency of the braking system based on the vehicle's mass, speed, braking distance, and braking time.

In this study, the efficiency of the tested vehicle's braking system was determined by measuring the stopping distance and braking time, which represents the novelty of this research (measuring the braking time). Additionally, measuring these parameters (distance and braking time) allowed for the validation of the efficiency of the vehicle's braking system used for research..

6.2 Materials and research methodology

he tested vehicle was also used in rural areas characterized by flat road routes at constant speeds, where the braking system was not heavily used but rather moderately. The chosen experimental vehicle, equipped with ABS and brake assistance devices, featured disc brakes and brake pads on both the front and rear axles (see Figure 5.4). The front axle had ventilated discs (see Figure 5.4a), while the rear axle had solid (non-ventilated) discs (see Figure 5.4b).

The testing of the braking system's efficiency was performed on a dynamometer at a speed of 5 km/h and a braking force of 6 kN, following the specifications provided in reference [23].

Therefore, the experimental procedure/methodology followed the same path as presented in Chapter 5 (the case of discs and brake pads used after covering 18,664 km, from 115,477 to 134,141 km). This chapter proposes the study of the behavior of the same vehicle's braking system with new discs and brake pads under heavy and moderate traffic conditions to enhance road safety by establishing its efficiency..

6.3 Experimental determination of the braking system's efficiency with new discs and brake pads

In order to determine the efficiency of the braking system, both the discs and brake pads were replaced with new ones. Previously, only the brake pads had been replaced, not the discs. After the earlier replacement of the original brake pads from the manufacturer with aftermarket pads, significant wear on the brake disc could be observed, underscoring the importance of using high-quality brake pads.

It is essential to note that the original brake disc was used with original brake pads for approximately 50,000 km. Subsequently, it was used for an additional 23,857 km with aftermarket brake pads. In Figure 6.1, the degree of wear on the brake disc can be observed (Figure 6.1).

The disc shows a relatively advanced stage of rust, as well as deep scratches across its entire surface. Due to the advanced wear of the brake disc, even though the brake pads were replaced 23,857 km ago (from 115,477 to 139,334 km), they experienced uneven wear. This justifies the previously demonstrated low efficiency of the braking system through tests on the brake stand.

In Figures 6.1 and 6.2, you can observe the uneven wear of the brake pads both on the front and rear axles..

Fig. 6.1 Uneven wear of the brake pads on the front axle

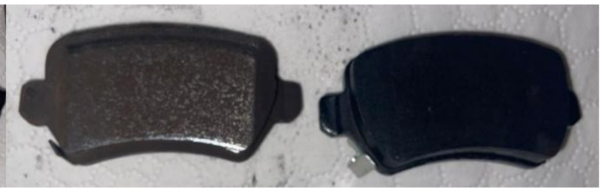

Fig. 6.2 Uneven wear of the brake pads on the rear axle

In order to determine the degree of wear on the front axle brake pads, a special gauge (Figure 6.3) was used.

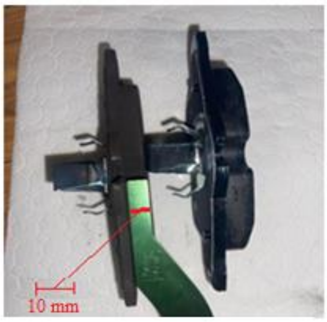

Fig. 6.3 The measurement of brake pad wear on the front axle

The thickness of the friction material on a new brake pad is 13 mm. For the worn brake pad, the gauge indicates a thickness of 10 mm, resulting in a wear of 3 mm over the 23,857 km traveled. For the rear axle brake pads, the thickness of the friction material on a new pad is 10 mm, and the gauge (Figure 6.5) indicated a thickness of 6.5 mm, resulting in a wear of 3.5 mm over the 23,857 km traveled.

Wear intensity, Iu, represents the amount of material lost/removed in thickness, hu (in mm), per unit of distance traveled (friction length - in this case, per kilometer). Thus, for both the front and rear axles, it will be determined using the formula [57]:

$$I_u = \frac{Initial\ thickness\ of\ the\ pad - remaining\ thickness}{Distance\ traveled\ (friction\ length)} = \frac{h_u}{L_f}, \tag{6.1}$$

Where: h_u - material thickness, in mm; L_f - wear length (distance traveled), in km.

Substituting the measured values, we get: $I_u = \frac{13mm - 10mm}{23.857\text{km}} \approx 125 \cdot 10^{-6} \frac{mm}{km}$.

In another form, the degree of wear can be expressed as a coefficient, k_u, or as a percentage, k_u , %:

$$k_u = \frac{Initial\ thickness\ of\ the\ pad - remaining\ thickness}{Initial\ thickness\ of\ the\ pad}, \tag{6.2}$$

Calculating, results: $k_u = \frac{13mm - 10mm}{13\text{mm}} \approx 0{,}23$ sau $k_u, \% = \frac{13mm - 10mm}{13\text{mm}} \times 100 \approx 23{,}08\ \%$.

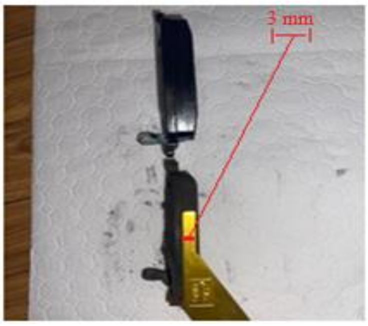

Fig. 6.5 The measurement of brake pad wear on the rear axle

Proceeding similarly and for the rear axle, applying the same relationships (6.1) and (6.2), we obtain:

$I_u = \frac{10mm-6{,}5mm}{23.857\text{km}} \approx 0{,}146 \cdot 10^{-6}\ mm/km$; $k_u = \frac{10mm-6{,}5mm}{10\ mm} = 0{,}35$ or $k_u, \% = 35{,}00\ \%$.

It is observed that the wear of the front axle brake pads (0.125 x 10^-6 mm/km or 23.08%) is lower than that of the rear axle (0.146 x 10^-6 mm/km or 35.00%), which is debatable due to the different levels of stress/usage. This means that the lifespan of the front axle brake pads is longer than that of the rear axle, which contradicts reality. Therefore, this highlights the need for further research and experiments. To address this, the discs (Fig. 6.4) and brake pads were replaced with new ones (Fig. 6.5). Additionally, the brake fluid was replaced, and the brakes were bled to achieve optimal pressure in the braking system.

Fig. 6.4 Worn brake disc

Fig. 6.5 New disc and pads assembly

The testing of the service brake and parking brake was conducted under the same conditions and in the same manner as previously described in Chapter 5. Additionally, the arrangement of the vehicle on the testing stand remained unchanged (see Figs. 5.8 - 5.10).

The results of the experimental trials led to the determination of the braking system's efficiency, along with other key parameters. These are presented in Tables 6.1, 6.2, and 6.3.

Table 6.1 Results obtained from the tests - Test 1

Parameter	Unit of measurement	Admissible limit	Measured Value
Total braking force of the service brake.	kN	-	10.38
Total braking force of the parking brake.	kN	-	3.44
Difference in braking force of the service brake.	%	30	13
Efficiency of the service brake, relative to the total mass of the vehicle.	%	50	71
Efficiency of the parking brake, relative to the total mass of the vehicle	%	16	23

Table 6.2 Results obtained from the tests - Test 2

Parameter	Unit of measurement	Admissible limit	Measured Value
Total braking force of the service brake.	kN	-	10.42
Total braking force of the parking brake.	kN	-	3.50
Difference in braking force of the service brake.	%	30	12
Efficiency of the service brake, relative to the total mass of the vehicle.	%	50	72
Efficiency of the parking brake, relative to the total mass of the vehicle	%	16	24

Table 6.3 Results obtained from the tests - Test 3

Parameter	Unit of measurement	Admissible limit	Measured Value
Total braking force of the service brake.	kN	-	10.42
Total braking force of the parking brake.	kN	-	3.28
Difference in braking force of the service brake.	%	30	11
Efficiency of the service brake, relative to the total mass of the vehicle.	%	50	71
Efficiency of the parking brake, relative to the total mass of the vehicle	%	16	22

6.4 Experimental results regarding the braking distance and time in relation to the vehicle's speed

A. Worn brake discs and pads

To facilitate comparison, the braking time and distance were determined as a function of the vehicle's speed (in two situations: the vehicle with worn brake discs and pads and the same vehicle with new brake discs and pads). A series of successive tests were conducted in the field.

It is worth mentioning that all values presented correspond to emergency braking, taking into account only the actual braking distance and time, excluding reaction time/distance since the brake pedal actuation point was established prior to the tests. At the time of conducting the tests, the vehicle had a mass of 1524 kg:

a) For speeds ranging from 20-25 km/h, the experimental results are shown in Figure 6.6, which displays graphical representations of braking time and distance as a function of speed.

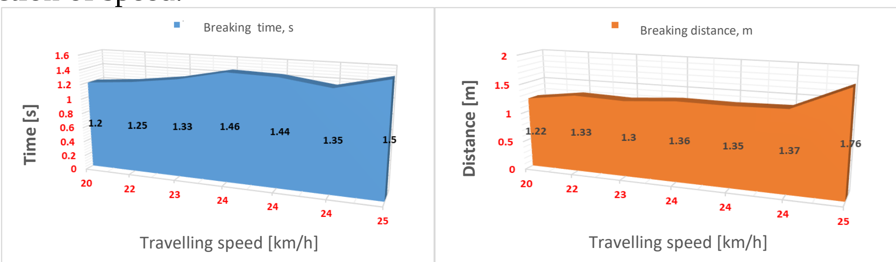

Fig. 6.6 Variation of braking time and distance as a function of travel speed between 20-25 km/h

b) For speeds ranging between 37-40 km/h, the experimental results are depicted in Figure 6.7, showing graphical representations of braking time and distance as functions of speed.

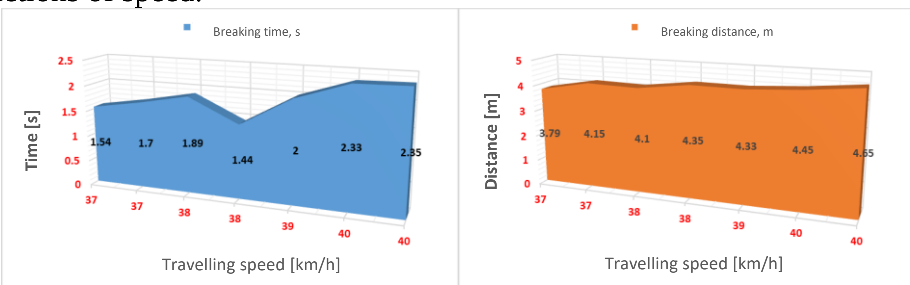

Fig. 6.7 Variation of braking time and distance as a function of travel speed between 37-40 km/h

c) For speeds ranging between 50-51 km/h, the experimental results are presented in Figure 6.8, showing graphical representations of braking time and distance as functions of speed

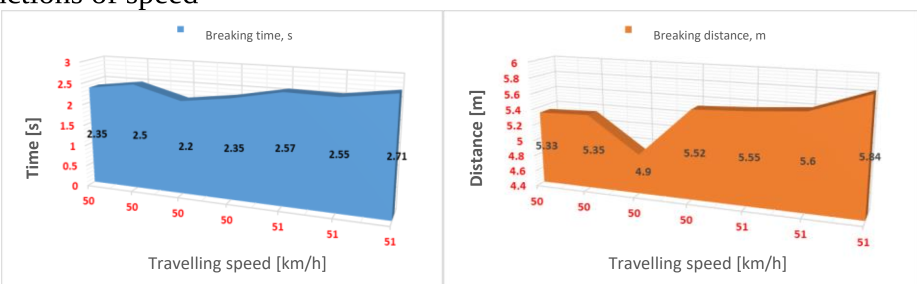

Fig. 6.8 Variation of braking time and distance as a function of travel speed between 50-51 km/h

B. New brake discs and pads

To determine the braking time and distance as a function of the vehicle's speed (equipped with new brake discs and pads), a series of successive tests were conducted in the field. At the time of conducting these tests, the vehicle had a mass of 1484 kg. As such;

a) For speeds ranging between 20-25 km/h, the experimental results are presented in Figure 6.9, showing graphical representations of braking time and distance as functions of speed.

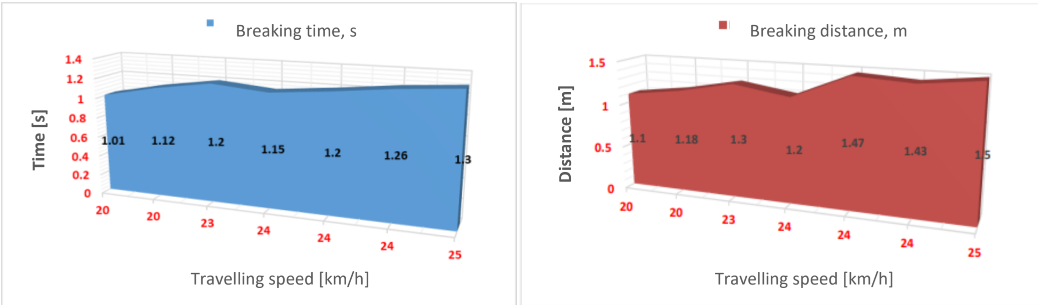

Fig. 6.9 Variation of braking time and distance as a function of travel speed between 20-25 km/h

b) For speeds ranging between 37-40 km/h, the experimental results are shown in Figure 6.10, depicting graphical representations of braking time and distance as functions of speed.

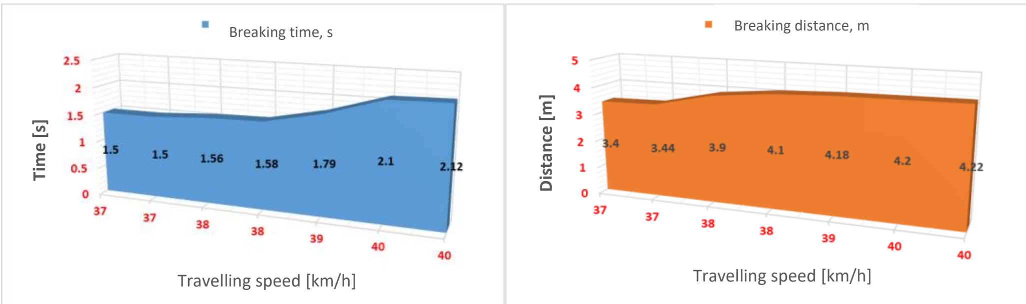

Fig. 6.10 Variation of braking time and distance as a function of travel speed between 37-40 km/h

c) For speeds ranging between 50-51 km/h, the experimental results are displayed in Figure 6.11, illustrating graphical representations of braking time and distance as functions of speed.

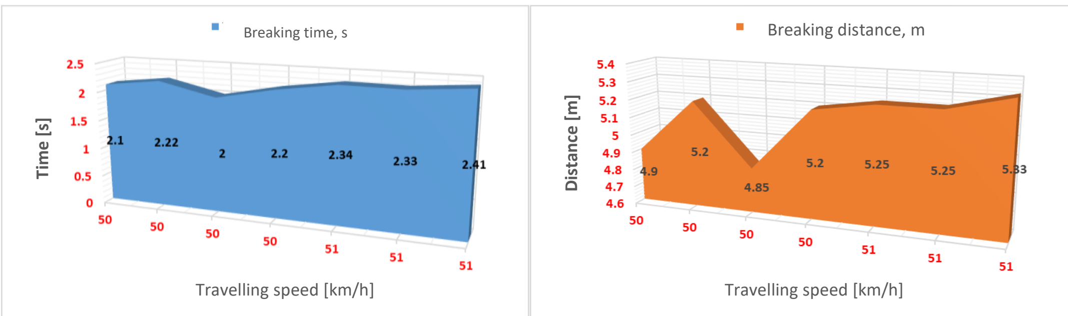

Fig. 6.11 Variation of braking time and distance as a function of travel speed between 50-51 km/h

6.5. Experimental results regarding the braking system efficiency after covering 10,553 km in heavy traffic.

6.5.1. Experimental results obtained on the testing stand

It is important to note that the vehicle was predominantly driven in the urban area, subject to heavy traffic. In this context, the braking system is one of the most heavily used components of the vehicle. Out of a total of 10,553 km traveled, 8,000 km were conducted in urban conditions, highlighting the intensity of using the braking system in such conditions.

In Figure 6.12, you can see the difference between the surface of the original disc from the manufacturer (Figure 6.12a) and the surface of the aftermarket disc. At the time of the test, the original disc had been used for approximately 50,000 km with original brake pads, while the aftermarket disc (Figure 6.12b) had been used for approximately 10,553 km with aftermarket brake pads. It can be observed that the aftermarket disc shows much more advanced degradation, despite being used for a shorter distance, emphasizing the importance of choosing high-quality discs and brake pads.


(a)


(b)

Fig. 6.12 The degree of wear on the brake discs:
a) original brake disc b) aftermarket brake disc

After covering 10,553 kilometers, the vehicle's braking system underwent a new set of tests to assess the performance and integrity of its components. These tests took place on a brake dynamometer, a specialized instrument that measures braking forces and provides detailed information about the efficiency and safety of the system. This evaluation is essential to ensure that the braking system is operating at optimal parameters and to identify signs of wear or damage.

I. Test 1:

Similar to the previous testing methodology, the vehicle was weighed to determine the parameters of the braking system.

Centralized results - Test 1

The essential parameters of the braking system were measured during the conducted tests and are presented in Table 6.4..

Table 6.4 Results obtained from the tests– Test 1

Parameter	Unit of measurement	Admissible limit	Measured Value
Total braking force of the service brake.	kN	-	14.98
Total braking force of the parking brake.	kN	-	9.55
Difference in braking force of the service brake.	%	<=30	3.20
Efficiency of the service brake, relative to the total mass of the vehicle.	%	>=50	3
Efficiency of the parking brake, relative to the total mass of the vehicle	%	>=16	21

<u>II.</u> <u>Test 2</u>:

Similar to the testing methodology used previously, the vehicle was weighed to determine the parameters of the braking system. The vehicle was placed on the brake dynamometer rollers, simulating a speed of 5 km/h. The brake was repeatedly activated to ensure precise results that reflect the real behavior of the system. A sensor was attached to quantify the force applied to the brake pedal.

Centralized Results - Test 2

The fundamental parameters of the braking system were determined from the conducted tests and can be viewed in Table 6.5..

Table 6.5 Results obtained from the tests– Test 2

Parameter	Unit of measurement	Admissible limit	Measured Value
Total braking force of the service brake.	kN	-	9.43
Total braking force of the parking brake.	kN	-	3.19
Difference in braking force of the service brake.	%	<=30	4
Efficiency of the service brake, relative to the total mass of the vehicle.	%	>=50	63
Efficiency of the parking brake, relative to the total mass of the vehicle	%	>=16	21

<u>III.</u> <u>Test 3</u>:

After establishing the vehicle's parameters, tests were conducted on the braking system on both axles. The vehicle was placed on the brake dynamometer rollers, simulating a speed of 5 km/h. The brake was repeatedly activated to ensure precise results that reflect the most realistic behavior of the system. A sensor was attached to quantify the force applied to the brake pedal.

Centralized Results - Test 3

The fundamental parameters of the braking system were determined from the conducted tests and can be viewed in Table 6.6.

Table 6.6 Results obtained from the tests– Test 3

Parameter	Unit of measurement	Admissible limit	Measured Value
Total braking force of the service brake.	kN	-	10.11
Total braking force of the parking brake.	kN	-	3.25
Difference in braking force of the service brake.	%	<=30	7
Efficiency of the service brake, relative to the total mass of the vehicle.	%	>=50	65
Efficiency of the parking brake, relative to the total mass of the vehicle	%	>=16	22

6.5.2 Rezultate experimentale privind distanța și timpul de frânare in funcție de viteza de deplasare a autovehiculului – discuri și plăcuțe uzate

a) *The degree of brake pad wear after 10,553 km. Statistical estimation of brake pad wear*

To statistically estimate the wear over time of the braking system, the vehicle was periodically driven for distances of 10 km under both intense and moderate traffic conditions. This revealed an average number of brake applications as follows:
- 42 light brake applications
- 27 moderate brake applications
-14 hard/abrupt brake applications.

Observing a total of 83 brake applications over 10 km, we can estimate the wear per 10,000 km as follows:

- Light brake applications: 42 × 1000 = 42,000 brake applications/10,000 km.
- Moderate brake applications: 27 × 1000 = 27,000 brake applications/10,000 km.
- Hard/abrupt brake applications: 14 × 1000 = 14,000 brake applications/10,000 km.

We consider the wear units factor k', with a value as close as possible to the maximum allowable, for each brake application (determined experimentally and recommended by the manufacturer, k' = 0.2 ... 0.9) based on:

- Light brake applications: k' = 0.3
- Moderate brake applications: k' = 0.6
- Hard/abrupt brake applications: k' = 0.9

Calculating the number of wear units:
(42000 × 0.3) + (27000 × 0.6) + (14000 × 0.9) = 12,600 + 16,200 + 12,600 = 41,400 units.
This means that the degree of wear will be:

$$k', \% = \frac{Number\ of\ wear\ units}{Maximum\ number\ of\ wear\ units} \times 100 \quad (6.3)$$

where *the maximum number of wear units* is *165,000*, representing the total allowed wear of the brake pads according to the manufacturer.

Replacing these values, we obtain: $k' = \frac{41.400}{165.0000} \times 100 = 25{,}09\ \%$.

b) The calculation of the actual wear degree of the brake pads

The new brake pads have a thickness of 13 mm on the front axle and 10 mm on the rear axle. After measuring with the gauge, it was observed that the worn pad has a thickness of approximately 10 mm on the front axle and approximately 7 mm on the rear axle, resulting in a wear of 3 mm after a distance of 10,553 km.

On the other hand, the new pads have a thickness of 10 mm on the rear axle. After measuring with the gauge, it was observed that the worn pad has a thickness of approximately 7 mm, resulting in a wear of 3 mm. Uniform wear is observed, but it is concerning given the number of kilometers traveled (10,553 km). In this case, the wear intensity, I_u, according to the equation (6.1), will be:

- for the front axle: $I_u = \frac{13\ mm - 10\ mm}{10.553\ km} \approx 284 \cdot 10^{-6} \frac{mm}{km}$, and

- for the rear axle: $I_u = \frac{10\ mm - 7\ mm}{10.553\ km} \approx 284 \cdot 10^{-6} \frac{mm}{km}$.

The wear coefficient, k_u according to equation (6.2), will be:

- for the front axle: $k_u = \frac{13mm - 10mm}{13\ \text{mm}} \approx 0.284$, and the wear degree (percentage).

$k_u = \frac{13mm - 10mm}{13\ \text{mm}} \times 100 \approx 28.42\%$;

- for the rear axle, we will have: $k_u = \frac{10mm - 7mm}{10\ \text{mm}} \approx 0.284$,

respectively: $k_u = \frac{10mm - 7mm}{10\ \text{mm}} \times 100 \approx 28.42\%$.

Statistical analysis showed that the aftermarket brake pads have a wear coefficient/factor of 25.09% and a wear intensity of 284·10^(-6) mm/km. In absolute terms, this translates to a real wear rate of 28.42% after 10,553 km traveled, or a wear intensity of $284 \cdot 10^{-6} \frac{mm}{km}$. This difference can be explained by several factors that influence the lifespan of a brake pad, including driving style, road conditions, and vehicle load..

c) Experimental results regarding braking distance and time in relation to the vehicle's speed

After covering approximately 10,553 km and conducting experiments on the testing stand, the vehicle underwent a series of tests to determine braking distance and time, correlated with the braking system's efficiency of 63%, measured on the brake dynamometer.

The instruments used for experimentation included a stopwatch, tape measure, and the vehicle's diagnostic system to monitor the exact speed. Markers were used to record the moment when the brake pedal was engaged. For testing purposes, the vehicle was brought to the desired speed and then set on autopilot to maintain that speed. Using the reference standard, the thickness of the brake pad substrate on both the front and rear axles was measured.

c1) for speeds ranging between 20-25 km/h, the experimental results are shown in Figure 6.13, which displays graphical representations of braking time and distance as functions of speed.

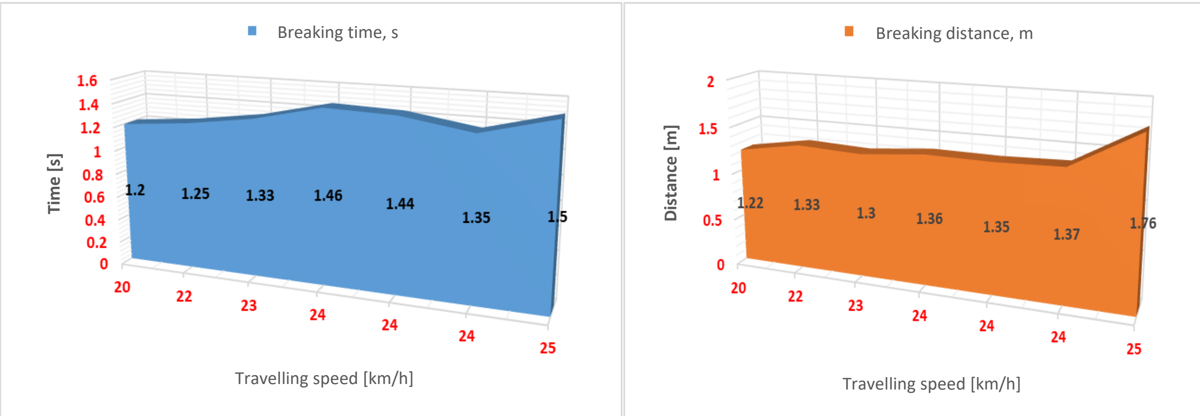

Fig. 6.13 Variation of braking time and distance as a function of travel speed between 20-25 km/h after covering the distance of 10.553 km

c2) for speeds ranging between 37-40 km/h, the experimental results are presented in Figure 6.14, which displays graphical representations of braking time and distance as a function of speed..

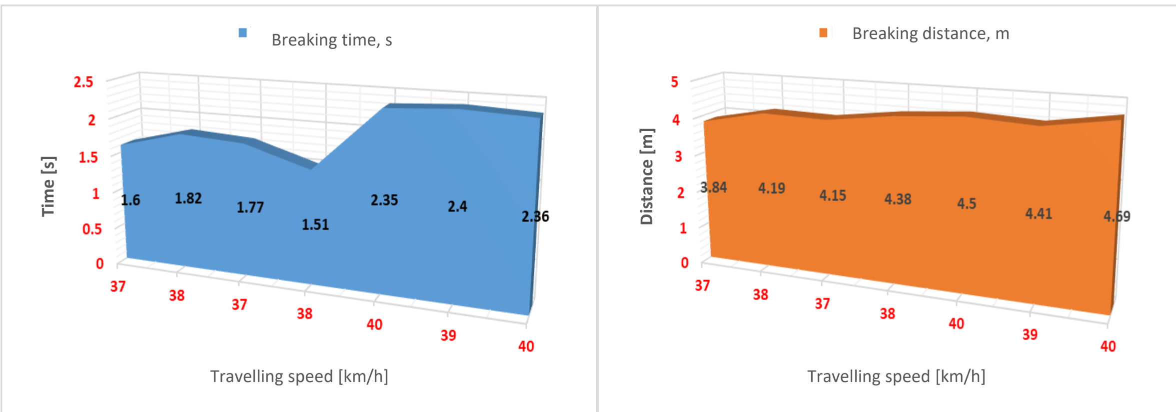

Fig. 6.14 Variation of braking time and distance as a function of travel speed between 37-40 km/h after covering the distance of 10.553 km

c3) for speeds ranging between 50-51 km/h, the experimental results are presented in Figure 6.15, which displays graphical representations of braking time and distance as a function of speed.

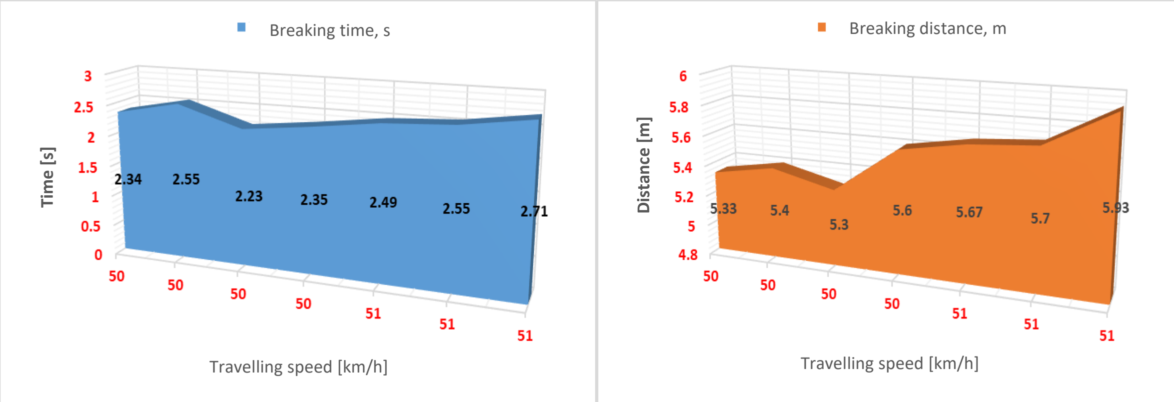

Fig. 6.15 Variation of braking time and distance as a function of travel speed between 50-51 km/h after covering the distance of 10.553 km

The calculation of the coefficient of friction

For determining the coefficient of friction, we will use the braking force measured on the dynamometer, taking into account the vehicle's mass,

m = 1524 kg (see Table 5.15. from thesis)

From 5.18 (found in thesis), we have the total braking force of the service brake:

F_f = 8,88 kN, though

$$F_f = \mu \times F_N, \tag{6.4}$$

$$F_N = m \times g, \tag{6.5}$$

where: μ - coefficient of friction, F_N – normal force, m – vehicle mass (1524 kg – from table 5.15 in thesis), g = 9,81 ≈ 10 m/s^2.

Calculation the normal force:

$$F_N = 1524 \times 10 = 15240\ N$$

From equation (6.4), results:

$$\mu = \frac{F_f}{F_N}. \tag{6.6}$$

Replacing the values, we get::

$$COF = \mu = \frac{8.880\ \mathrm{N}}{15240,} = 0.582$$

The obtained coefficient of friction, μ (COF), with a value of approximately 0.582, indicates the relationship between the braking force and the weight of the vehicle on the road.

A coefficient of 0.582 is a reasonable value and falls within the typical range for braking a vehicle on dry asphalt.

This value suggests good tire grip on the road surface, which is essential for efficient and safe braking.

Similarly, the COF can be calculated for each braking force of the vehicle, corresponding to different masses, both measured on the brake dynamometer.

These values are presented in Table 6.7, along with the evolution of the braking system's efficiency and the measured braking force, based on the vehicle's mass (considering masses of 1,480, 1,484, 1,514, and 1,524 kg) and the number of kilometers driven (115,477; 134,141, 139,334, 149,887), and graphically represented in Figure 6.16..

Table 6.7 Braking System Efficiency Based on Weight and Kilometers Driven

	Vehicle mass 1480 kg- 115477 km	**Vehicle mass 1524 kg - 134141 km**	**Vehicle mass 1484 kg - 139334 km**	**Vehicle mass 1514 kg - 149887 km**
Braking force for the service brake (kN)	9.14	8.88	10.38	10.06
Braking force for the parking brake (kN)	2.94	2.91	3.44	2.71
Difference in braking for the service brake (m)	5	5	12	8
Efficiency of the service brake, relative to the total vehicle mass (%)	71	59	72	63
Efficiency of the parking brake, relative to the total vehicle mass (%)	16	19	24	21
Coefficient of friction (COF)	**0,617**	**0,582**	**0,699**	**0,664**

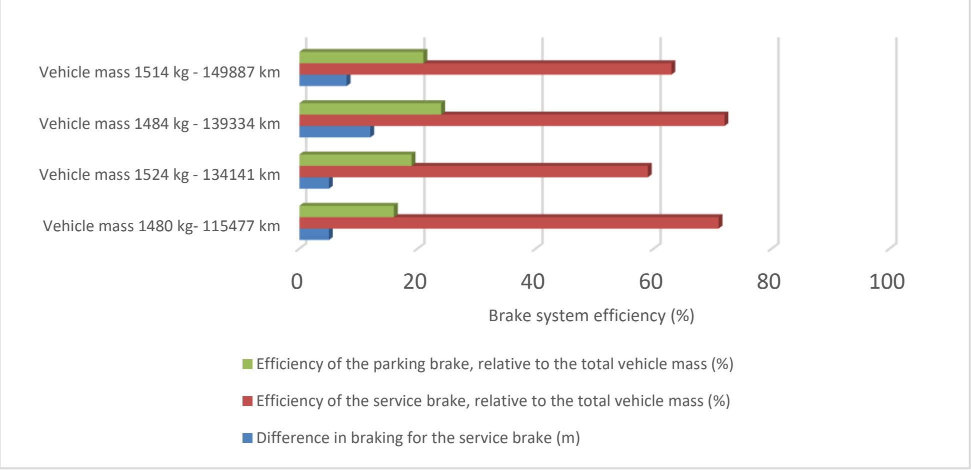

Fig. 6.16 Evolution of the braking system efficiency depending on the vehicle's mass and traveled kilometers

Furthermore, in Figure 6.17, the evolution of the COF (Coefficient of Friction) in relation to the braking force and the vehicle's mass, as measured on the brake dynamometer, is presented.

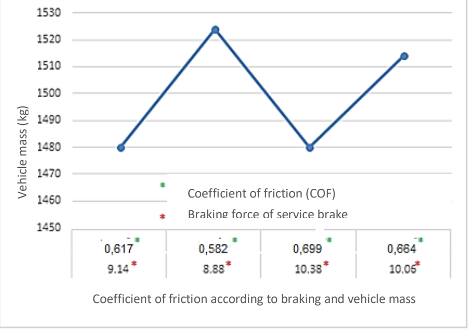

Fig. 6.17 The evolution of the coefficient of friction (COF) in relation to the total force of the service brake and the vehicle's mass

To determine the COF following an emergency stop through calculation, you will use the equations for uniformly decelerated motion based on the velocity of the vehicle. [57]:

$$u = -a \cdot t = d \cdot t, \qquad (6.7)$$

where: u - initial velocity (considering u = 40 km/h, which is equivalent to 11.11 m/s after converting from km/h to m/s), t - braking time (2.35 s in this case – see Table 6.14 from thesis), a - acceleration in m/s^2. d - deceleration, which is negative in the case of braking, expressed in m/s^2:

$a = -\,d = -\frac{u}{t}$, therefore d = u/t. (6.8)

Replacing the measured values for the speed of 40 km/h and braking time of 2.35 seconds, we obtain:

d = (11,11/2,35) = 4,727 m/s^2.

Then, we know that the deceleration (negative acceleration) is:

a = - d = - μ·g, resulting d = μ·g, (6.9)

g - the acceleration due to gravity, and it has a value of approximately 9.81≈ 10 m/s^2, μ - COF. Therefore, the coefficient of friction, COF = μ, can be determined from equation (6.9) as:

$\mu = -\frac{a}{g} = \frac{d}{g}$ (6.10)

Results $\mu = \frac{4{,}727}{10} = 0.472$.

Therefore, a very good COF within the recommended range of 0.3 - 0.7 by literature, designers, and automobile manufacturers for calculations in brake system design. The negative values are purely conventional and indicate deceleration. The real COF (without the negative sign) is approximately 0.472. Similarly, the COF will be calculated for each speed of the vehicle at the moment of braking, corresponding to a measured braking efficiency on the brake dynamometer and presented in Table 6.8 and Figure 6.18

Table 6.8 Distance, braking time, and COF (Coefficient of Friction) based on braking system efficiency and speed

	Braking System Efficiency, %	Vehicle speed, km/h	Braking time, s	Braking distance, m	COF
Brake system with worn discs and pads	59	25	1.5	1.76	0.463
		40	2.35	4.65	0.472
		50	2.5	5.35	0.555
Brake system with new discs and pads	72	25	1.3	1.5	0.534
		40	2.12	4.22	0.524
		50	2.22	5.2	0.625
Brake system with worn aftermarket discs and pads	63	25	1.58	1.79	0.439
		40	2.36	4.69	0.470
		50	2.55	5.4	0.544

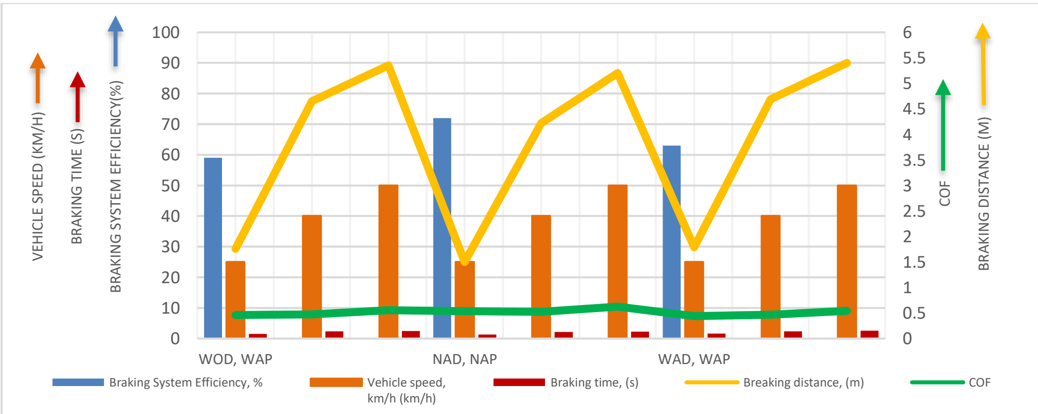

Fig. 6.18 Comparison between braking times and distances measured for the worn brake system and the new brake system: WOD - worn original disc; WAP - worn aftermarket pads; NAD - new aftermarket disc; NAP - new aftermarket pads; WAD - worn aftermarket disc

Figure 6.19 shows the evolution of COF (Coefficient of Friction) as a function of traveling speed corresponding to the brake system efficiency according to Table 6.8.

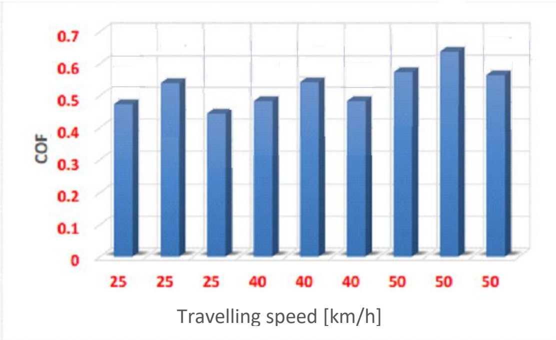

Fig. 6.19 Figure 6.19 shows the evolution of COF (Coefficient of Friction) as a function of traveling speed corresponding to the brake system efficiency according to Table 6.8

It can be observed that the evolution of COF alternates in a similar pattern with the vehicle's traveling speed. On average, it increases with the rising speed when the braking efficiency is at 59%, after which it follows a nearly insignificant decrease when the braking efficiency is at 72% (see Table 6.8). This pattern repeats for a braking efficiency of 63% as well (see Figure 6.18).

Speeds, distances, braking times, and COF were compared for both the worn brake system with DOU + PUA and the new brake system with DNA + PNA, as well as for the worn brake system with DUA + PUA. Under normal vehicle load conditions (1524 kg), a braking system efficiency of only 59% was observed. Considering that the minimum acceptable braking system efficiency is 50% (see Table 6.8), these results are concerning and suggest the need for replacing the braking system at a much shorter interval than recommended..

6.6. 3D finite element numerical simulation study of the car braking system and the friction pair of disc brake pads

6.6.1 3D numerical simulation with finite element analysis

The wear of the friction material is one of the important characteristics of brake pads. Good brake system performance is closely associated with the quality of the material, as well as operational safety, and is therefore directly related to the brake's lifespan [133, 134].

A 3D finite element numerical model of the car's brake system was used for friction and wear analysis using the ANSYS Workbench R16 software. The model considered the brake pad and brake disc as viscoelastic materials.

The 3D geometric model of the brake system was designed using SOLIDWORKS, and coupled thermal and structural analysis was performed using the ANSYS Workbench R16 software.

The brake was applied when the car was traveling at 51 km/h (ω = 54.5 rad/s), and the braking duration until the car stopped was approximately $t \approx 2.5$ s. For the given example, the average COF during braking, considering the pressure on the brake pad p = 4.5 MPa, was μ = 0.4.

It should be noted that the simulation program was extended to a speed of 87.5 km/h (ω = 125 rad/s), braking time t = 5 s, brake pad pressure p = 7.5 MPa, and μ started at 0.35, values that also match those measured during the tests (as presented above).

The mechanical characteristics and dimensions of the gray cast iron disc brakes and the selected brake pad materials in the analysis are presented in Table 6.9.

Table 6.9. Material Characteristics and Dimensions of the Brake Disc and Brake Pad

Dimensions / Properties	**Disk**	**Pad**
Inner Diameter (mm)	61	170.2
Outer Diameter (mm)	260.0	258
Thickness (mm)	22.0	15
Density (kg/m3)	7200	2030
Mass (kg)	4.71	0.230
Young's Modulus (MPa)	210000	3180
Poisson's Ratio	0.28	0.35
Coefficient of Thermal Expansion (mm/°C)	$1{,}1\cdot10^{-5}$	$3{,}1\cdot10^{-6}$
Thermal Conductivity (W/K.m)	37	0.275

To generate finite element meshes, a 3D tetrahedral method will be used. In general, 85,856 nodes and 44,867 contact elements are used for the disc and brake pads, as shown in Figure 6.20..

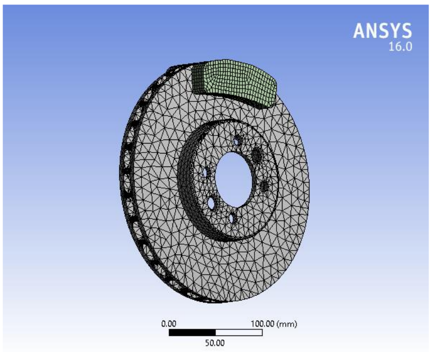

Fig. 6.20 Capture of the mesh with ventilated disc.

A. Simulation Model. Boundary Conditions

For the simulation, boundary conditions are required as follows: The coefficient of friction (COF) for the contact pair (disc-brake pads) is 0.4; the initial temperature was 22°C; the disc material is gray cast iron; along with the geometric dimensions and material properties of the disc and brake pad, as listed in Table 6.9. The wheels are decelerated from a traveling speed of 51 km/h (54.5 rad/s) and 87.5 km/h (125 rad/s) to a final speed of 0 km/h in 2.5 s and then 5 s, and mechanical energy is converted into thermal energy. A braking pressure of 4.5 and 7.5 MPa is applied to the brake pad to generate the braking force. The boundary conditions applied to the simulation model of the disc and brake pad geometry are illustrated in Figure 6.21.

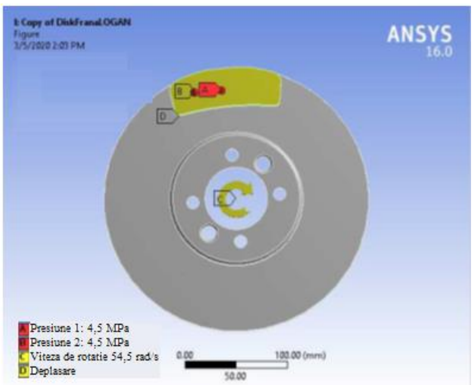

Fig. 6.21 Boundary conditions in the simulation program - disc brake with brake pads

B. Analysis of deformation and stresses in the brake disc and brake pad

From the deformation analysis of the disc shown in Figure 6.22, it can be observed that the total displacement of the brake pad is 0.312 mm (Figure 6.22(b)), which is relatively close compared to the disc's displacement of 0.417 mm (Figure 6.22(a)).

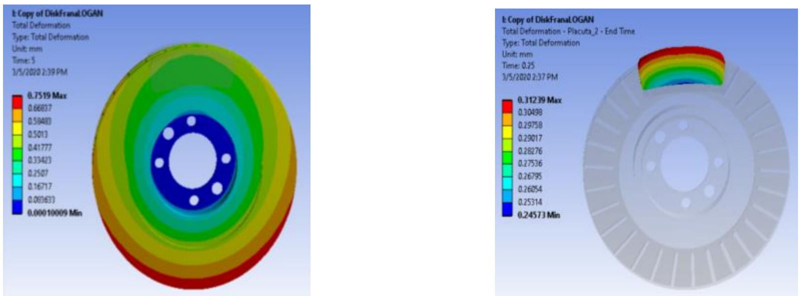

(a) (b)

Fig. 6.22 The distribution of the total displacement on the disc and brake pad: (a) Displacement of the disc.(b) Displacement of the brake pad.

The analysis of the mechanical stress of the disc, as shown in Figure 6.23 (a) and (b), presents the distribution of the equivalent Von Mises stress at the end of the simulation (on the inner disc, Figure 6.23 (a), and on the outer disc, Figure 6.23(b)). The scale of values ranges from 1,335 to 344.65 MPa for the disc-brake assembly.

The maximum value of 344.46 MPa recorded during the simulations in the disc-brake pad pair occurs at the bowl/cavity of the disc. This is because the disc is fixed to the wheel hub by bolts, preventing its movement.

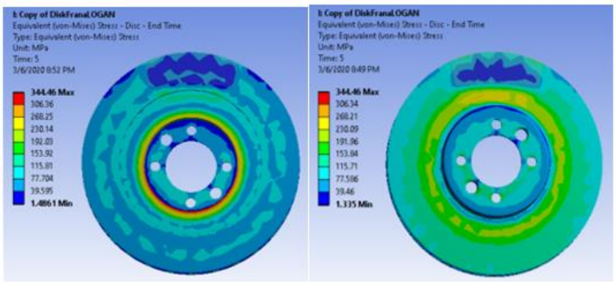

(a) (b)

Fig. 6.23 The equivalent (Von Mises) stress distribution on the inner disc (a) and the outer disc (b)

In brake systems, the sliding speed between the disc and the brake pads is variable (Fig.6.24). At low and very low speeds, the stick-slip phenomenon occurs due to the elasticity of the brake system components [139, 140]. The amplitude of this phenomenon is influenced by the stiffness characteristics of the brake system, the operating speed, and the friction behavior of the disc-brake pad material pair.

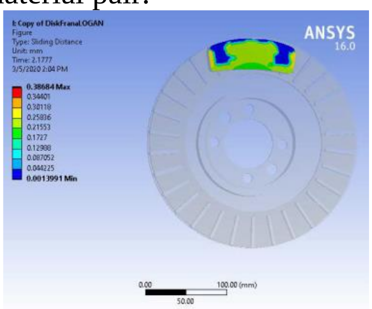

Fig. 6.24 The results outline the sliding distance for the disc-brake pad pair.

C. The analysis of the contact pressure distribution at the disc-brake pad interface

Figure 6.25 shows the contact pressure distribution at the friction interface of the inner brake pad at different simulation times. For this distribution, the scale ranges from 0 to 11.812 MPa and reaches a maximum value at t ≈ 2.5 s and t = 5 s, corresponding to the stopping of the vehicle. The distribution of the contact pressure on the disc surface exhibits a non-uniform load field at the surface contact with the brake pad.

The distribution of frictional stresses for the geometric model of the disc with the brake pad is presented in Figure 6.26. Considering that the model takes into account the sliding phenomenon, the resulting variation of the frictional stress is artificial..

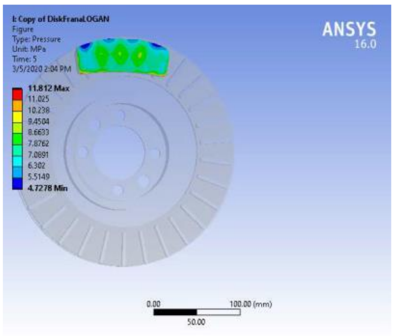

Fig. 6.25 Contact pressure distribution

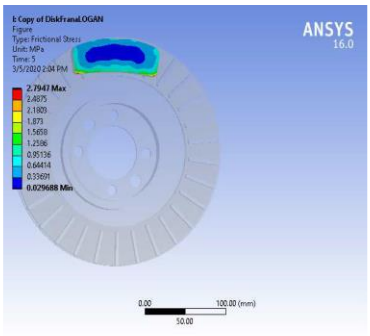

Fig. 6.26 Distribution of frictional stresses

D. Numerical simulation of wear at the brake disc-pad interface

The results of the simulations, in the form of volumetric wear evolution over time and the cumulative wear profile (total volumetric wear), are presented in Figure 6.27(a) and (b). The input data for solving the differential equation (6.13) with the initial condition $V_t(0) = 0$ were as follows: K_{disc} = 1066 (mm3/m), H_{disc} = 720 (MPa), K_{pad} = 906 (mm3/m), H_{pad} = 120.7 (MPa), and a time step Δt = 0.25 s..

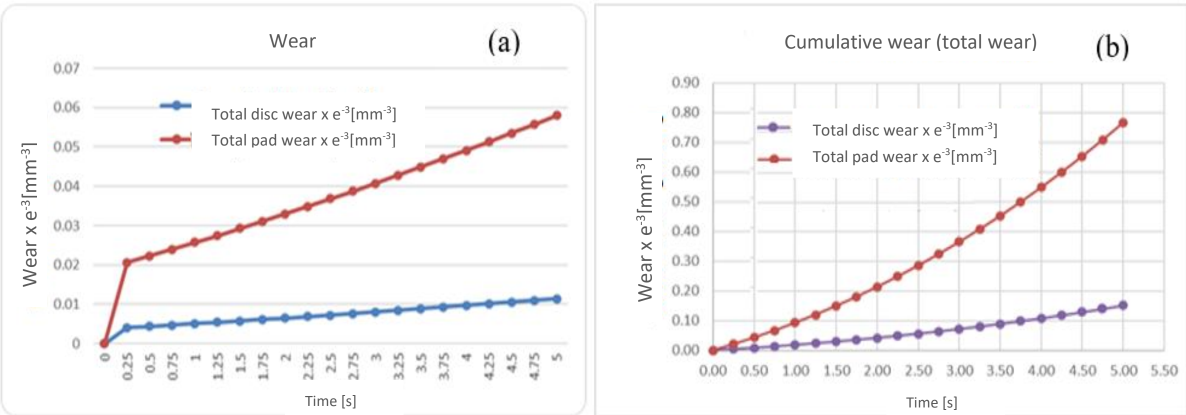

Fig. 6.27 Time evolution of volumetric wear (a) and total volumetric wear (b) obtained during braking, for disc (red line) and pad (blue line)

From the analysis of the tribological behavior of the braking system (disc-brake pads) of the tested car, through the finite element method, results can be obtained for the efficient design of the basic components of the braking system.

The contact pressure between the disc and brake pads is higher on the outer areas than on the inner areas of the pads, with the highest value being near the central axis of the outer area. Additionally, it can be observed that the wear of the brake pads is approximately five times greater than that of the brake disc..

6.6.2 Experimental evaluation of wear and COFof the disc-brake pad couple

For the experimental evaluation of COF and the intensity of wear of the disc-disc brake torque the tribometer was used. The disc samples were made from a disc with a diameter of 60 mm, and the plate samples are cylindrical sticks of 10 mm in diameter. The experimental tests, both for friction (COF) and for wear (volumetric wear intensity), were carried out under different conditions (Fig. 6.28): speed, constant contact pressure and temperature (FIG.6.28(a)); temperature at constant speed and constant contact pressures (Figur.6.29(b)); specific braking pressure at constant velocity and temperature(Figure 6.28(c) – for COF, respectively the volume wear intensities relative to the energy consumed by friction, constant speed, and constant touch pressure (Figu.6.27(d)). It is worth noting that COF and wear intensity values are average values.

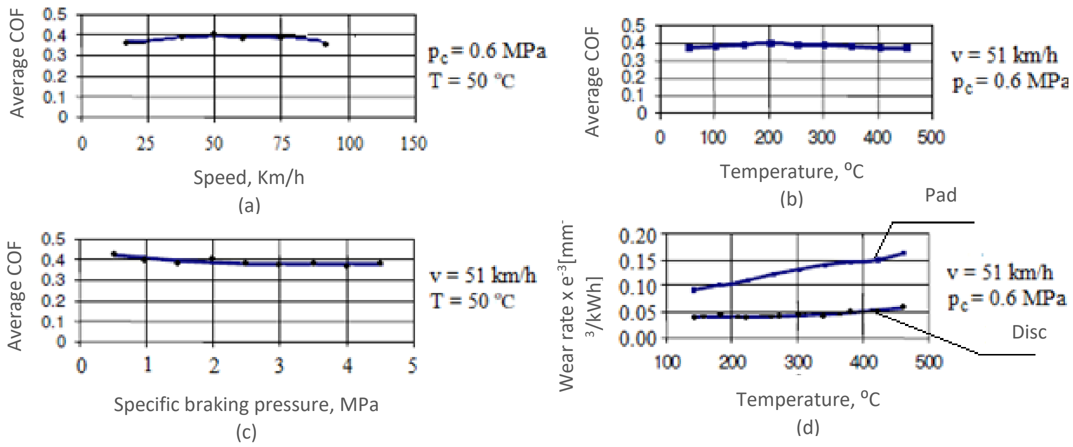

Fig. 6.28 COF variation according to speed (a), temperature (b), specific braking pressure (c) and volume wear intensity according to temperature (d),ining two other parameters constantly

It is observed that the COF variation is relatively constant (about 0.4) with very small variations. The COF variation with speed at constant contact pressure and temperature (see Fig. 6.28 (a)), starts from the approximate value of 0.36 - 0.37 at a relative speed of 20 km/h, then has a slight increase to the value of 0.4 - 0.42 at a speed of 50 km/h (where it reaches its maximum), after which it decreases relatively slightly with the increase in speed, because at the speed of 87.5 km/hr, the COF reaches the value from where it started (0,36 – 0,37). The COF variation with temperature at constant speed and contact pressure starts from an approximate value of 0.37 - 0.38 (see Fig. 6. 28 (b)), to a temperature of 50oC, followed by an increase to 200oC, where it reaches a maximum of 0.4 – 0.42 then start to decrease relatively slightly to the temperature of 450oC, when it reaches back to the original value of 0.37 - 0.38.

6.7 Modal analysis of the disc-brake brake system

6.7.1 Generalities

Modal analysis is a dynamic analysis, giving the natural frequencies at which a structure will resonate. These natural frequencies are of paramount importance in various fields of engineering [139]. In the automotive industry, suspension and braking systems are usually adjusted to have different natural frequencies for passenger cars and racing cars. The problem of braking systems demonstrates the friction contact of and uses its own complex solutions to predict unstable modes (noise, vibrations, etc.)

In Fig. 6.29 is schematically rendered how can be done modal analysis of the brake disc-plate assembly, by simulation of dynamic transit, harmonic, random vibrations and by response spectrum.

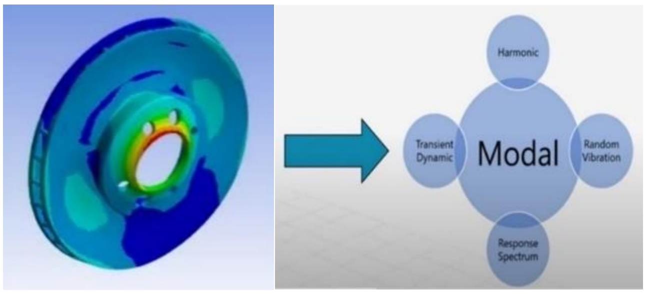

Fig. 6.29 Methods of modal analysis of the brake disc-plate assembly

A simple overview of the brake disc-plate model created with the 3D CAD program SolidWorks2022, Dassault Systèmes, USA is presented in Fig. 6.30. The disc is ventilated and has a total thickness of 22 mm, with a full (right-left) section of 10 mm, and the brake plates are 15 mm thick. The inner diameter of the disc is 61 mm, and the outer diameter is 260 mm. On this model a pre-tensioned modal analysis is performed using different methods to determine the unstable modes

Fig. 6.30 Brake disc-plate assembly

6.7.2 Contact and target pair modeling

Problems arising in the contact area of the brake disc-plate usually require manual calculations of asymmetrical terms deriving from sources such as friction sliding and then introducing asymetric terms using special elements (cum ar fi MATRIX27). The surface-surface friction contact pairs with a friction coefficient of 0.3-0.5 are used to define the contact between the brake plates and disk to simulate the friction slip contact that occurs at the plate-disk interface. The surface-to-surface contact pairs are also used to define the contact for other components that will always be in contact throughout the braking process. The contact and target pairs for the friction contact on both sides of the disc are shown in Fig. 6.31 (a) and (b).

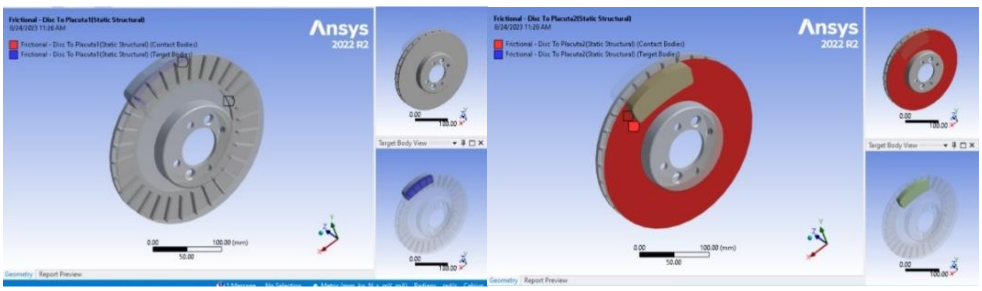

(a) (b)

Fig. 6.31 Contact pairs and target for friction contact disc-brake plates: (a) inner face (to the engine); (b) outer face (quad wheel)

For the friction contact pairs, the augmented Lagrange algorithm is used, because the pressure and friction stress are increased during the equilibrium iterations, so that the penetration is gradually reduced.

6.7.3 Generating internal sliding movement and the finite element network of the brake disc-plate pattern

For generating internal sliding motion, the CMROTATE command is applied which defines constant rotation speeds on the contact/target nodes. The specified rotation speed is used only to determine the sliding direction and has no effect on the final solution. Thus, the final discretized grid for the disc-brake brake assembly is shown in Fig. 6.32.

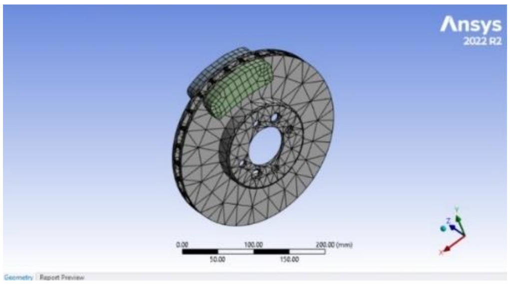

Fig. 6.32 Discretized end grid for brake disc-brake pad assembly

6.7.4 Conditions at the limit of movement and loading

After setting the discretization grid, the model load (Fig. 6.33) is reduced with restrictions regarding:
- the force due to the pressure of the heater, the wheel moment, the reaction due to wheel action on the lane and the angular (rotation) speed of the disc;
- the inner diameter of the disc hose and screw holes is narrowed in all directions;
- a small pressure is applied to both ends of the plate to establish contact with the brake disc and to include the pretension effects;
- the pressure is increased nominally to 7.5 MPa in two stages (the first is 4.5 MPa);
- the movement on the brake plate surfaces where pressure is applied is restricted in all directions except the axial direction (de-a lungul axei Z).

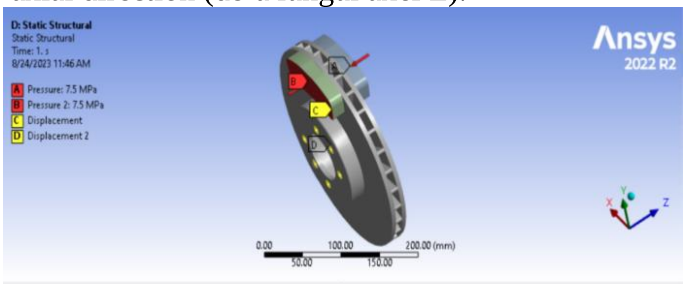

Fig. 6.33 Conditions at the limit of movement and loading

6.7.5 Modal analysis and control solutions

The complex modal analysis and solution control settings are carried out using the UNSYM resolution algorithm with the own UNSYM solution, as a method of non-compressed linear modal analysis. For this, the geometry of the brake assembly (brake disc-plates) is imported and the model is configured as above, respectively the contact rigidity matrix is based on its initial state and when the rigidization stress effects are not critical. Then the following modular analysis command fragment (CMROTATE) is inserted to generate the sliding friction force.

6.7.6 Mode participation factor

Naturally, in any analysis the question arises whether each natural frequency is equally important. For a real physical model, we could have thousands or millions of degrees of release (DOF), which means we can find just as many natural frequencies. For example, considering the case of the brake plate disc there is a very large number of DOFs, that is, as many frequencies and natural modes.

Thus, the participation factor, γ_i, for module i and temperature, T, will be:

$$\gamma_i = \{\Phi\}\{\Phi\}_i^T[M]\{D\}\ , \qquad (6.11)$$

where: $\{\phi\}$ – mode shape; [M] – the mass matrix; {D} – the direction of the excitation vector, and the actual mass of the module i, is:

$$M_{ef,\,i} = \gamma_i^2\ , \qquad (6.12)$$

that is, the square of the participation factor is the actual mass. In some specialty papers, the actual mass is even called the participation factor, γ. The participation factor, γ and effective mass, Mef have similar roles in modal analysis.

Variation of solving time by modal analysis is shown in Figure 6.34

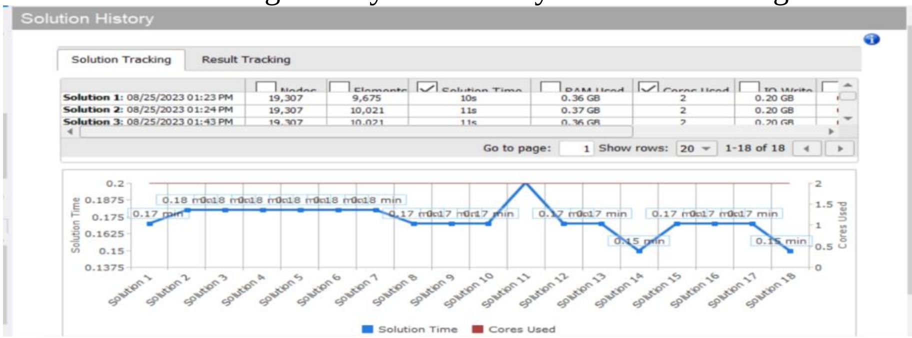

Fig. 6.34 Variation of solving time by modal analysis

6.7.7 Results and discussions

The unstable predictions for the brake disc-plate assembly using both methods were very close, due to the relatively small precompression load. The non-compressed linear modal solution predicted unstable modes at 6474 Hz, while the completely disturbed non-linear model foresaw unstability at 6458 Hz.

Five motor vehicle speeds were chosen, along with the maximum speed required by design, as being the most common. In each case analysed 6 frequencies were determined at which the mechanical structure enters into resonance in increasing order, the first being determining in establishing the efficiency of the structural integrity of the disc (see Table 6.10)..

Table 6.10 Scenarios analysed at different speeds of the vehicle

Scenario analyzed	Angular speed (rad/s)	Moving speed (km/h)
1	60.38	50
2	96.60	80
3	150.9	125
4	217.4	180
5	265.7	220

If the disc reaches resonance, depending on the frequency at which it resonates, it deforms from the original structure by up to 47 mm, in which case the maximum stress in the piece reaches the value of 50,965 MPa, Fig. 6.35.

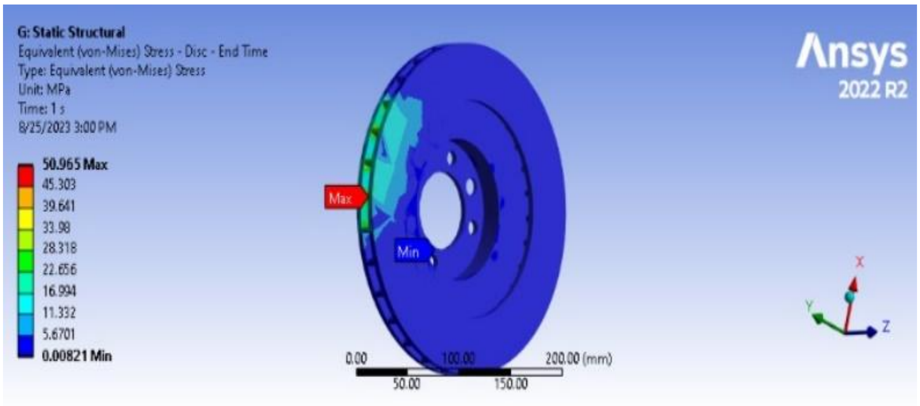

Fig. 6.35 Disc voltage state, vibration mode 2, scenario 2

The frictional stress at different travel speeds and different COF values is presented in Table 6.11 and 6.12.

Table 6.11 Frictional Stress at Different Vehicle Travel Speeds

The analyzed scenario	Viteza unghiulară (rad/s)	Friction-Induced Stress (MPa)	Frictional Stress Distribution
1	60.38	0.3361	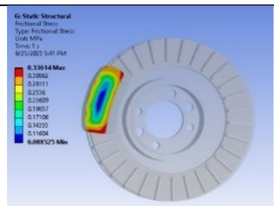
2	96.60	0.3365	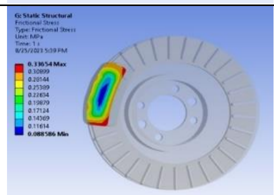
3	150.9	0.3383	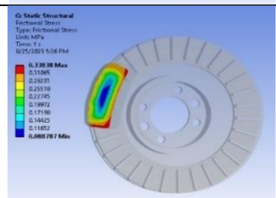
4	217.4	0.3528	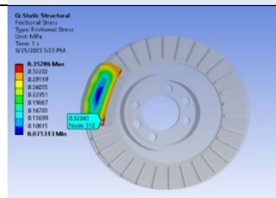
5	265.7	0.3697	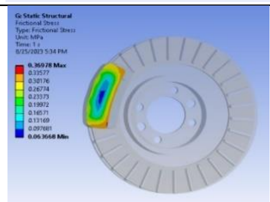

Table 6.12 Frictional Stress at Different Coefficient of Friction Values

The analyzed scenario	**Coefficient of Friction (μ)**	**Frictional Stress (MPa)**	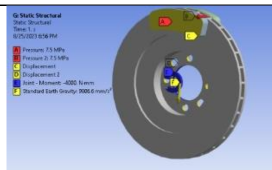
1	0.2	0.3357	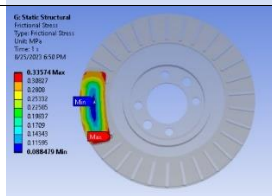
2	0.25	0.409	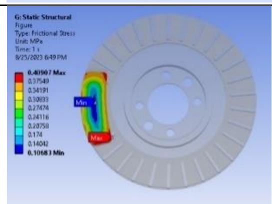
3	0.3	0.4789	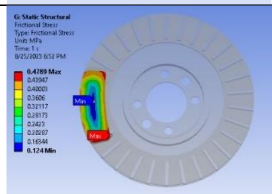
4	0.35	0.5454	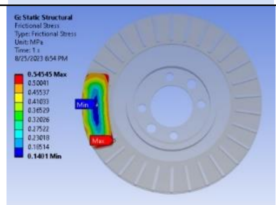
5	0.4	0.6089	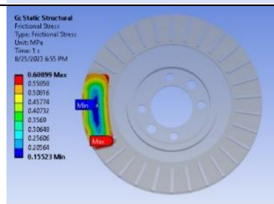

Therefore, the results obtained from the simulations confirm the possibility of introducing modal analysis into the design process, as well as advancing experimental research on the vibration behavior of the brake disc and optimizing it in this regard. From the estimated values and graphical representations obtained from the simulations, it can be concluded that the rotational speed of the disc at which it vibrates at the resonance frequency (equivalent to over 1650 km/h) is much higher than the speed it experiences during operation, indicating the structural integrity of the disc..

Conclusions

There are many studies and research based on models that closely mimic reality; however, there are few that incorporate real-time data from operation. Experimental results have been validated through experimental testing methods as close to operational reality as possible, including data sampling during operation.

This applies particularly to brakes and braking systems, which need to be tested and approved in accordance with various regulations and safety standards related to road safety. Following experimental tests, a significant decrease in the efficiency of the braking system was observed after just 18,664 km of operation under both heavy and moderate traffic conditions.

The braking system of the tested vehicle was evaluated according to the current regulations and safety standards for road safety. There are situations where, under normal vehicle load but with brake pads and discs that have covered 18,664 km under heavy and moderate traffic conditions, the efficiency of the braking system is slightly above the minimum acceptable point (50%). As a result, these findings are worrisome, indicating the need for brake system replacement at a much shorter interval than recommended.

After replacing the worn discs and brake pads, it was found that the braking system's efficiency increased by 14% (from 59% to 73%). Following the replacement with new aftermarket discs and pads, the vehicle covered 10,553 km under heavy traffic conditions. The braking system's efficiency decreased to 63%, and a pad wear rate of 28.42% was observed. These results are concerning and emphasize the importance of using quality brake discs and pads, as well as the impact of heavy traffic on the braking system.

The experimental tests showed that recommendations regarding the frequency of disc and brake pad replacement are inconsistent with the actual wear of the braking system. It is necessary to study the parameters of a new brake system to estimate its wear over time. After testing the vehicle's braking system in the field, the system will be replaced, and tests on the new braking system will be conducted to determine its efficiency. The determination of braking system efficiency was based on measuring braking distance and time as a function of vehicle mass, speed, and kilometers traveled.

It was found that the relative deformations of the brake pads and disc are greater in the outer diameter zone than in the inner diameter zone. This is due to the fact that the contact pressure between the brake disc and pads is higher on the outer zones than on the inner zones of the pads, with the highest value near the central axis of the outer zone.

Within the scope of statistical analysis, a discrepancy was identified between the theoretically calculated wear rate and the actual wear rate of aftermarket brake pads. Over the course of 10,000 km, a theoretical wear rate of 25.09% was obtained, while the actual measurement indicated a wear rate of 28.42%. This difference can be explained by several factors influencing the lifespan of brake pads, including driving style, road conditions, and vehicle load. Therefore, it is recommended to perform regular and detailed measurements to obtain a clearer and more precise picture of the wear rate, allowing for proper adaptation of the vehicle's maintenance strategy, thus ensuring a longer lifespan and increased safety.

To study the structural characteristics and tribological behavior of a vehicle's braking system, a simulation program was developed using ANSYS Workbench. The results obtained through finite element analysis provide reference values for the structural selection of materials used in designing a more efficient brake system with disc and pad structures. Additionally, the numerical research results have shown that an increase in contact pressure and/or relative velocity between contact surfaces leads to an increase in the amplitude of the stick-slip phenomenon.

Significant improvements in work efficiency and reduced design time are observed through the use of software such as ANSYS Workbench. Additionally, brake pad wear is several times greater (approximately five times) than brake disc wear. Simultaneously, experimental results correlate with theoretical ones, justifying and validating the research methods used in this thesis..

Chapter 7. GENERAL CONCLUSIONS. PERSONAL CONTRIBUTIONS. FINAL CONCLUSIONS. RECOMMENDATIONS AND PERSPECTIVES.

7.1. General conclusions

Tribology, the science of studying friction, wear, and lubrication, plays a vital role in understanding the performance and reliability of any mechanical system. In the automotive field, where safety is of the utmost priority, the tribological behavior of the braking system provides critical insights into the efficiency and durability of this essential system. Studying the tribological behavior of the braking system under various traffic conditions has become imperative due to the complexity and diversity of situations on modern public roads.

The study revealed some concerning findings, especially regarding aftermarket brake pads and discs. It appears that many of these aftermarket components do not meet the quality standards of original parts. As a result, they exhibit accelerated wear under heavy traffic conditions, which can lead to reduced brake performance and even potential dangerous situations in traffic. Moreover, inferior brake pads can produce excessive noise and decrease the overall efficiency of the braking system.

Recent research has shown that, under heavy traffic conditions, the wear of braking system components, especially pads and discs, is significantly accelerated. More alarmingly, many aftermarket components don't seem to adhere to the same quality standards as original parts. This can lead to reduced performance, increased noise, and most concerning, potential compromises in vehicle safety.

In light of these findings, there is a clear need for stricter regulations for aftermarket components and proper consumer awareness regarding the potential risks associated with using these products. They also highlight the necessity for ongoing tribological studies to monitor the evolution of production techniques and materials and ensure the safety of vehicles and their passengers on increasingly congested roads.

It's evident that there's an acute need to address these findings with seriousness and rigor. Tribological research must continue and deepen, monitoring the evolution of technology and materials. Only through understanding and adaptation can we hope to maintain a high level of road safety in today's traffic context. Additionally, consumers need to be educated about the importance of choosing quality components and the risks associated with using inferior quality parts.

Following a meticulous study that involved successive changes of braking system components and repeated monitoring of its performance, the significant impact of various factors, including heavy traffic, on braking efficiency can be highlighted.

At the beginning of the experiment, the braking system, consisting of the original worn disc and new aftermarket brake pads, showed an efficiency of 73%. As mileage accumulated, at 18,664 km, efficiency dropped to 59%, a phenomenon observed in the context of heavy traffic, which requires repeated and substantial use of the braking system. After recording 23,857 km, a complete replacement of the braking system with new aftermarket components was carried out, resulting in an efficiency increase to 72%. However, a different wear rate is noted between the front axle, at 25.09%, and the rear axle, at 14.676%, indicating the impact of heavy traffic and driving style on the differential wear of brake pads..

At a new checkpoint, 10,553 km later, the system's efficiency was assessed at 63%, with a wear rate of 28.42%. This new data set highlights the fact that heavy traffic continues to have a significant impact on braking efficiency, consistently and progressively stressing the braking system components.

The current study also focused on a detailed analysis of the structural characteristics and tribological behavior of the braking system, exploring these dimensions with the aid of a simulation program implemented in ANSYS Workbench R16. The finite element analysis, which was central to this research, facilitated the creation of a well-defined set of criteria for material selection. This scientific approach played a crucial role in conceptualizing an optimized braking system, with a pronounced emphasis on the disc and brake pad architecture.

The study also showed a disproportionate wear rate between the brake pads and the brake disc, establishing a ratio of five to one. This fact underscores the importance of more in-depth research into the materials used for brake pads to extend their lifespan and improve the overall efficiency of the braking system.

The significant advantages of using the ANSYS Workbench R16 software in the research process were demonstrated. Not only did it optimize the design process, reducing the required time, but it also provided a robust platform for the experimental validation of the methodologies adopted within this thesis. Moreover, it highlighted a remarkable consistency between theoretical data and experimental results, thus validating the reliability and accuracy of the obtained data. This shows that the use of advanced technologies can significantly improve precision and efficiency in developing safer and more reliable braking systems.

In conclusion, heavy traffic played a decisive role in the fluctuations of the braking system's efficiency, imposing accelerated and differentiated wear on its components. The implementation of a regular maintenance and monitoring regime is vital to ensure an optimal level of safety and performance under conditions of intense and variable traffic. Considering these findings, it is recommended to perform periodic checks on the braking system, especially in the context of a dynamic driving style and complex traffic conditions.

7.2. Personal contributions

In the context of the doctoral thesis, the aim was to expand knowledge in the field of braking system performance, placing special emphasis on the influence of usual components under different traffic conditions. A fundamental aspect of my research was the practical approach, geared towards real traffic, in contrast to most existing studies that largely rely on laboratory results. The details of the contributions are presented below:

<u>Analysis of the braking system under traffic conditions (on the field)</u> - considering that most research in this area is conducted in the laboratory, I chose to study the braking system under real traffic conditions. This helped me obtain a more realistic perspective on the performance and wear of components.

<u>Study on the use of worn original discs and new aftermarket pads</u> - under real traffic conditions, I evaluated the efficiency and wear rate of the system using this specific combination. The results highlighted interactions between aftermarket components and worn original ones.

<u>Full assessment of the aftermarket system in heavy traffic</u> - I analyzed the performance of a braking system fully equipped with new aftermarket discs and pads. This study was vital for identifying potential issues related to the quality of braking system components.

<u>Statistical estimation of pad wear</u> - I simulated and analyzed the wear rate of brake pads under heavy and moderate traffic conditions, observing the braking trend over a distance of 10 km.

<u>Monitoring critical parameters -</u> I closely monitored and analyzed essential parameters such as the degree of wear, friction coefficient, wear rate, braking distance, and time. These measurements provided a clear picture of the impact of speed and efficiency on performance.

Finite element analysis - modeling and detailed analysis of the braking system using the finite element method/analysis can help determine benchmark parameters when choosing braking system materials.

Integration/correlation of experimental results from dynamometer testing - although the emphasis was on field (on-ground) research, I also included dynamometer tests to validate and complement my conclusions from the real-world environment.

Through this combined approach, my research provided an innovative and comprehensive perspective on braking systems. It underscores the need for a balanced approach between laboratory research and real-world conditions to gain a complete understanding of this crucial field of automotive engineering.

7.3. Final conclusions.

In the conducted research, we examined the tribological behavior and mechanical performance of the braking system, comprised of the original, already worn brake disc, and new aftermarket pads. From the initial analysis, the braking system's efficiency determined by dynamometer methods showed a value of 73%. Intriguingly, after a distance of 18,664 km, dynamometer data indicated a significant drop in efficiency, recording 59%. This decline also manifested in the physical condition of the disc, which, at 23,857 km, showed damage in the form of deep scratches, a clear sign of suboptimal compatibility with the inferior quality aftermarket pads. Wear assessments indicated values of 25.09% for the front axle and 14.676% for the rear axle.

The statistical analysis of the braking system, conducted over a distance of 10 km, considering various traffic conditions, revealed valuable information regarding the system's behavior and wear in real-time. Observing the number of brakes and behavior in traffic, we can conclude that braking systems exhibit increased wear risk under heavy traffic conditions compared to moderate traffic. This analysis underscores the need for proactive maintenance strategies and possibly developing more durable braking systems to ensure optimal functioning and increased safety under the varied traffic conditions encountered in practice.

Following these preliminary results, we proceeded to replace the system with new components, aiming to investigate the behavior of an entirely new system under similar conditions. Regrettably, after only 10,553 km in heavy traffic, the pads again showed evident signs of relatively accelerated wear. Moreover, the wear coefficient of the pads reached a value of 28.42%, and the overall efficiency, evaluated dynamometrically, recorded a new decline, standing at 63%.

The experimental data highlighted a strict correlation between the braking system's efficiency and vital parameters, such as braking distance, braking time, and friction coefficient. These correlations, evidenced in an advanced academic context, bring to the forefront the imperative of ongoing research in the braking field and underscore the vulnerabilities in using aftermarket components. In heavy traffic conditions, these relationships become even more pronounced, underlining the crucial importance of component selection and continuous research.

The study tackled the structural characteristics and tribological behavior of the braking system through a simulation program implemented in ANSYS Workbench. The finite element and modal analysis, applied in this research, facilitates defining selection criteria for the materials used, thereby contributing to designing a more efficient braking system, with a particular emphasis on the disc's structure and brake pads.

The results indicate an amplification of the stick-slip phenomenon in the context of increased contact pressure and/or relative speeds between contact surfaces. It is also noteworthy that there's significantly higher wear of the brake pads compared to the brake disc, with a ratio of about five to one..

Additionally, several important conclusions can be highlighted:

1. Evaluation of the braking system's efficiency:

- There's a notable degradation in the braking system's efficiency over a relatively short range of km (18,664 km and 10,553 km respectively), suggesting that component wear may be faster than initially anticipated under heavy and moderate traffic conditions.
- Replacing worn brake pads and discs significantly improves the braking system's efficiency, with an increase of 14%.

2. Performance parameters and their variability:

- Contact pressure is higher in the outer area of the discs, making that zone more prone to wear.
- A slight discrepancy exists between theoretical and actual wear rates, particularly in the case of aftermarket brake pads. This can be attributed to the unpredictability of the materials used and external factors like traffic, driving style, weather conditions, etc.

3. Using ANSYS Workbench R16 software:

- The use of the ANSYS Workbench software not only optimized efficiency and shortened the design process duration but also allowed for experimental validation of the research methodologies adopted in this thesis, highlighting a notable concordance between theoretical and experimental data.
- The software significantly assisted in modeling and analyzing the tribological behavior and structural characteristics of the braking system, providing critical benchmark values in material selection and design.
- Results suggest that increased pressure and/or speed can amplify the stick-slip phenomenon, emphasizing the importance of focusing on these parameters in braking system development.

4. Impact of heavy traffic:

- Heavy traffic not only impacts the braking system's efficiency but also driver behavior, underscoring the need for a highly efficient braking system.
- There's an acute need for ongoing research in the field of braking system behavior under heavy traffic conditions to ensure better road safety.

5. Correlation between theoretical and experimental data:

- Experimental results validate and justify the research methods used in the thesis, showing a good correlation with theoretical data.
- A zig-zagging trend in the friction coefficient (COF) evolution was observed, varying based on several factors, including vehicle weight and braking force.

6. Vehicle maintenance recommendations:

- Regular and detailed checks of the wear rate are recommended, allowing for appropriate adjustments to the vehicle maintenance strategy for longer lifespan and increased safety.
- Current recommendations regarding the frequency of replacing brake discs and pads might be inadequate, indicating a need for revisiting them to more accurately reflect the actual wear observed in experiments.

7. Implications for future design:

- The findings suggest that there's significant room for improving the current design of braking systems, involving different material choices or structural modifications to reduce wear and enhance efficiency..

- The experience gained from this study can be instrumental in guiding future developments in this field, contributing to the creation of optimal braking systems.

The results of this doctoral thesis illustrate not only the need for a rigorous scientific approach in evaluating and selecting braking components (original disc - aftermarket pads, aftermarket disc - aftermarket pads), but also the disproportionate impact of heavy traffic on their durability and performance. These achievements emphasize the imperative of adopting higher standards in the production of aftermarket components and a deep understanding of the dynamics of heavy traffic on braking systems, thus contributing to the safety and efficiency of road traffic.

In conclusion, the current study proves to be essential in the context of changing dynamics of modern traffic. The findings underscore the importance of regular and attentive maintenance, as well as the judicious selection of components, to guarantee optimal efficiency and increased long-term safety. It is vital to understand that current traffic realities impose a new standard for road safety studies, and thus, this research significantly contributes to updating and adapting our knowledge in this crucial domain..

7.4. Recommendations and Perspectives (Future Research Directions)

Deepening Research on Materials for Brake Pads and Discs - In light of our data, there is a clear need to explore and develop new materials or combinations of materials that better withstand the high demands of intense traffic. Investigating composition, heat treatments, or manufacturing technologies may reveal more durable and efficient alternatives.

Continuous Investigation in Intense and Moderate Traffic Conditions - The data clearly shows that intense traffic accelerates component wear compared to moderate traffic. It is crucial to continue research under these conditions to better understand the relationship between traffic intensity and brake system performance. The approach should not be limited to the laboratory but should also include tests in real conditions to capture the real dynamics and complexity of traffic and road situations.

Artificial Intelligence and Real-Time Monitoring - There is immense potential in integrating artificial intelligence (AI) for real-time monitoring of brake system parameters. An AI system can collect and analyze real-time data, such as friction coefficient, temperature, and wear, providing instant and predictive feedback to drivers and mechanics.

Predictive Alert Systems - Using advanced algorithms, AI can be trained to recognize wear patterns and anticipate potential failures, issuing alerts before they become critical.

Advanced Simulations - While real-world testing is essential, increasing technology and computing power can be used to create advanced simulations. These can replicate various traffic and wear conditions, allowing researchers to anticipate and adapt to challenges before they arise in reality.

Education and Awareness - It is essential to educate the general public and the automotive industry about the importance of correct component selection and the risks associated with using inferior quality aftermarket components.

Industry-Academic Collaboration - Partnerships between academic institutions and the industry can lead to significant innovations, combining practical expertise with fundamental research.

In summary, intense and moderate traffic significantly influence the performance and durability of braking systems. Given this finding and potential implications for road safety, the emphasis on research under these conditions and the integration of modern technology becomes essential for the evolution and optimization of braking systems.

SELECTIVE BIBLIOGRAPHY

[1]	W. Post, „Car braking systems," in: K. Reif, eds) *Car braking-system components. Function, Regulation and Components*, Wiesbaden, Springer Vieweg, 2014, pp. 28-29, DOI://doi.org/10.1007/978-3-658-03978-3_3.
[2]	C. A. Cimpeanu și I. S. Cimpeanu, Automobilul: Siguranța rutieră și poluarea, Resita: Editura Tim, 2019.
[3]	R. Stefan-Ionescu, Optimizarea constructiva și ecologica a componentelor sistemului de franare al autoturismelor, Brasov: Universitatea Transilvania din Brasov, 2019.
[4]	K. Reif, „Car braking-system components," in K. Reif, *Brakes, Brake Control and Driver Assistance Systems. Function, Regulation and Components*, Wiesbaden, Springer Vieweg, 2019, pp. 28-39.
[6]	O. Maluf, M. Angeloni, M.T. Millan, D. Spinelli, W,W.B. Filho, „Development of materials for automotive disc brakes", *Pesquisa Technol Minerva,* 2004, vol. 4, nr. 2, pp. 149-158.
[7]	A. Rashid, Overview of Disc Brakes and Related Phenomena - a review, *International Journal of Vehicle Noise and Vibration* 2014, 10(4), 257-301, http://dx.doi.org/10.1504/IJVNV.2014.065634.
[10]	.J. Abutu, .S.A. Lawal, M.B. Ndaliman, R.A. Lafia Araga, „An overview of brake pad production using non–hazardous reinforcement materials," A*cta technica corviniensis – Bulletin of Engineering* , vol. 3, nr. XI, 2018.
[12]	*** Textar, „https://textar.com/wp-content/uploads/2016/02/TX_BRO_PC-FaultDiagnostics_A4_RUM_WEB.pdf".
[23]	O. Câmpian, Gh. Ciolan, Dinamica Autovehiculelor, Brasov: Editura Universitatii Transilvania din Brasov, 2001.
[24]	N.A. Stoica, A. Tudor, „Experimental results about the stick-slip phenomenon with application to the disc-brake friction materials couple used in the automotive domain," *UPB Scientific Bulletin, Series D: Mechanical Engineering* , vol. 1, nr. 80, 2018.
[25]	E. Denimal, J-J. Sinouac, S. Nacivet, „Influence of structural modifications of automotive brake systems for squeal events with kriging meta-modelling method," *Journal of Sound and Vibration*, vol. 463(22), 2019, https://doi.org/10.1016/j.jsv.2019.114938.
[27]	B. Novaković, M. Kavalić, S. Stanisvljev, M. Vlahović, S. Boric „The Importance of Application and Maintenance of Braking System in Modern Automobile," in *VI International Conference Industrial Engineering and Environmental Protection 2016*, Zrenjanin, Serbia, 2016.
[32]	F. Ilie, A.C. Cristescu "*Tribological Behavior of Friction Materials of a Disk-Brake Pad Braking System Affected by Structural Changes—A Review*", Materials 2022, *15*(14), 4745, WOS:000832109100001, https://doi.org/10.3390/ma15144745.
[52]	Childs P.R. *Mechanical Design Engineering Handbook,* Chapter 13 - Clutches and Brakes 2014, Butterworth-Heinemann, 513-564, https://www.sciencedirect.com/book/9780080977591/mechanical-design-engineering-handbook.
[53]	I. Hutchings, S. Philip, „9 - Applications and case studies," in *Tribology (Second Edition),*, Butterworth-Heineman, 2017, pp. 303-352, https://doi.org/10.1016/B978-0-08-100910-9.09984-0.
[54]	A. Day, „Chapter 2 - Friction and Friction Materials," in *Braking of Road Vehicles*, Butterworth-Heinemann, 2014, pp. 9-34, https://doi.org/10.1016/C2011-0-07386-6.
[57]	Ilie F., **Cristescu A.C.** "*Experimental Study of the Correlation between the Wear and the Braking System Efficiency of a Vehicle*", Appl. Sci. 2023, *13*(14), 8139, https://doi.org/10.3390/app13148139.

[60]	G. Riva, **F. Varriale, J.Wahlstrom,** „A finite element analysis (FEA) approach to simulate the coefficient of friction of a brake system starting from material friction characterization", Friction 9, 2021 pp. 191-200, https://doi.org/10.1007/s40544-020-0397-9.
[62]	*** Abaqus, „Information about Abaqus," [Interactiv]. Available: https://www.3ds.com/productsservices/simulia/products/abaqus/.
[64]	P. Chen, „Performance, The Testing and Data Analyzing of Automobile Braking", *International Conference on Computational Science and Engineering* 2015, pp. 440-444, DOI: 10.2991/iccse-15.2015.82.
[65]	*** Dewesoft, „Vehicle Brake Test and ABS Testing", [Interactiv]. Available: https://dewesoft.com/applications/vehicle-testing/brake-test.
[66]	Ryme, „Brake tester for Light & Commercial Vehicles FRL 5.5", [Interactiv]. Available: https://www.ryme.com/en/producto/brake-tester-for-light-and-semi-industrial-vehicles-frl-5-5/.
[67]	*** Tribonet, „Tribometer", [Interactiv]. Available: https://www.tribonet.org/tribometer/.
[71]	D. Berjoza, V.P. Ilmars Dukulis I. Jurgena, „Testing automobile braking parameters by varying the load weight", in *TAE*, Prague, 2019.
[75]	A. Demira și A. Oz, „Evaluation of vehicle braking parameters by multiple regression method," *Scientia Iranica B*, vol. 6, nr. 26, pp. 3334-3355, 2019, DOI: 10.24200/SCI.2019.51584.2262..
[77]	M. Kchaou, A. Sellami și e. al, „Friction characteristics of a brake friction material under different braking conditions," *Mater. Des*, vol. 52, pp. 533-540, 2013.
[79]	P. Mădălin-Florin și B. Nicolae-Vlad, „Study of Brake System Parameters for Commercial Vehicles," in *Proceedings of the 4th International Congress of Automotive and Transport Engineering (AMMA 2018)*, 2018.
[84]	S. B. Sarip, Lightweight friction brakes for a road vehicle with regenerative braking. Design analysis and experimental investigation of the potential for mass reduction of friction brakes on a passenger car with regenerative braking., University of Bradford, 2011, http://hdl.handle.net/10454/548.
[88]	Cristescu A-C., Ilie F., Ipate G.,Voicu1 Gh., Stefan V. Studies and research on the tribological behavior of the braking systems of vehicles. Review, *E3S Web of Conferences 286, 03021 TE-RE-RD* 2021, https://doi.org/10.1051/e3sconf/202128603021.
[94]	Filip I., **A.C. Cristescu -** *Experimental Study of the Correlation between the Wear and the Braking System Efficiency of a Vehicle*, Appl. Sci. 2023, *13*(14), 8139, https://doi.org/10.3390/app13148139.
[106]	J. Tang, D. Bryant și H. S. Qi, „Coupled CFD and FE Thermal Mechanical Simulation of Disc Brake," in *EuroBrake 2014*, Lille, France, 2014.
[107]	A. Demir și A. Oz, „Evaluation of vehicle braking parameters by multiple regression method," *Scientia Iranica B*, vol. 6, nr. 26, pp. 3334-3355, 2019, http://2014.eurobrake.net/proceedings.
[109]	*** https://www.vehiculedufutur.com/Brochure_ROTOTEST.
[114]	F. Talati, S. Jalalifar, "Analysis of Heat Conduction in a Disk Brake System", *Heat and Mass TransferJ* vol. 45, 1047- 1059, 2009. DOI: 10.4236/epe.2011.32018.
[115]	*** Brake &Front End, " The Real Cost of Installing Cheap Brake Pads", https://www.brakeandfrontend.com/the-real-cost-of-installing-cheap-brake-pads/.
[116]	Nussbaum, Break Test Standas, Test Lanes and Headlight Testers. *Passenger Cars and Transporters* 2016, http://13154129.s21d-13.faiursd.com.
[139]	G. Ipate, **A.C. Cristescu**, C.D.Cotici, N.E Gheorghiță, D. Ionescu, A.F. Hristache, Evolution of tribological behavior of a brake disc-pad friction pair using a fizzy inference model based on an adaptive network (ANFIS), 11th International Conference on Thermal Equipment Renewable Energy and Rural Development (TE-RE-RD 2023, Bucharest, Romania.

CURRICULUM VITAE EUROPASS	europass
PERSONAL INFORMATION	
Surname / First Name	**CRISTESCU ANDREEA CĂTĂLINA**
EDUCATION AND TRAINING	
Period	2019-present
Educational Institution	*Polytechnic University of Bucharest,* *Doctoral School of Biotechnical Systems Engineering*
Degree Obtained	Ph.D. Student
Field of Study	Mechanical Engineering
Period	2017-2019
Educational Institution	*Polytechnic University of Bucharest,* *Faculty of Biotechnical Systems Engineering*
Degree Obtained	Master's Degree
Field of Study	Mechanical Engineering
Period	2013-2017
Educational Institution	*Polytechnic University of Bucharest,* *Faculty of Biotechnical Systems Engineering*
Degree Obtained	Engineering Degree
Field of Study	Environmental Engineering
Period	2009-2013
Educational Institution	*"Radu Greceanu" National College, Slatina, Olt*
Degree Obtained	Baccalaureate Diploma
Field of Study	Natural Sciences
PROFESSIONAL EXPERIENCE	
EMPLOYER	Idemia Technologies România, București, România
Period	2021- prezent
Type of Activity	Information & Technology
Position Held	Software Integration Engineer (DevOps)
Position Held	Test and Integration Engineer
EMPLOYER	Impeda SoftDev - Bricsys (Hexagon), București, România
Period	2019-2021
Type of Activity or Business Sector	Information & Technology
Position Held	Software Tester & Analyst
EMPLOYER	AKKA Romserv, București, România
Period	2019-2019
Type of Activity	Automotive
Position Held	Mechanical Engineer/ Design Engineer
EMPLOYER	National Institute for Research and Development in Machines and Installations for Agriculture and Food Industry - INMA Bucharest, Romania

Period	2017-2019									
Type of Activity	Research and Development									
Position Held	Design Engineer, Scientific Research Assistant, Web Designer									
PERSONAL SKILLS AND COMPETENCIES										
Mother tongue(s)	Română									
Other language(s)	Engleză, Franceză									
European Level (*)	UNDERSTANDING				SPEAKING				WRITING	
	Listening		Reading		Conversational		Oral Presentation		Writting	
English	C1	Proficient User	C1	Proficient User	C1	Proficient User	C1	Proficient User	C1	Proficient User
French	B2	Independent User	B2	Independent User	A2	Basic User	A2	Basic User	B2	Independent User
Skills and Abilities	Linux, Docker, Kubernetes, SVN, Jenkins, Nexus, Sonar, VMWare, OpenStack, Bash shell, Ansible Oracle, Postgres Database, JBOSS/Wildfly, TestLink, Xray, Servicii web https, REST, SOAP, Jira, Confluence, Rabbit MQ, Active MQ, AWS, Zookeeper, Microsoft Office, Adobe Photoshop AutoCAD, BricsCAD, HTML5, CSS3, Boostrap4, SEO, Xray, Zephyr for Jira, Testrail, Azure DevOps, Azure, Redmine, OS X, GitHub, Catia V5/V6, Enovia									
Artistic Skills and Abilities	I attended violin and music theory courses for 7 years									
Communication Skills	I possess excellent communication skills, demonstrating the ability to build solid collaborative relationships and convey technical information in an accessible and efficient manner									
Driving License(s)	I have held a category B driver's license since 2012.									
ADDITIONAL INFORMATION										
Courses and Certifications	• "Entrepreneurship" - Politehnica Universityof Bucharest POSDRU program • "Hydraulics" - National Institute INOE • AZ-104 Microsoft Azure Administrator -Microsoft • ITIL® 4 Foundation – ITAcademy • Linux Command Line Essentials - Become a Linux Power User! – UDEMY • Oracle Database Architecture – UDEMY • Complete DevOps Ansible Automation Training – UDEMY • The Complete SSL and TLS Guide: HTTP to HTTPS – UDEMY • Azure Kubernetes Service (AKS) Made Easy: - UDEMY • Complete Linux Training Course to Get Your Dream IT Job 2023 – UDEMY • Jenkins, From Zero To Hero: Become a DevOps Jenkins Master – UDEMY • Bash Scripting and Shell Programming (Linux Command Line) – UDEMY • Docker Mastery: with Kubernetes +Swarm from a Docker Captain - UDEMY									
Publications	Author and co-author of 31 research articles, published in ISI & BDI rated international journals									
Books	Technical Equipment for Mechanized Maintenance of Vineyards: Lucreția POPA, Vasilica ȘTEFAN, Andreea Cătălina CRISTESCU									
Projects	I participated in 10 European Projects									
Conferences	I attended 15 International Conferences.									

PUBISHED PAPERS

A. Papers published in ISI-ranked journals

1. Filip Ilie, **Andreea-Catalina Cristescu**, Experimental Study of the Correlation between the Wear and the Braking System Efficiency of a Vehicle, *Applied Sciences* 13 (14), 8139, 2023.
2. F Ilie, **AC Cristescu**, A study on the tribological behavior of molybdenum disulfide particles as additives, *Coatings* 12 (9), 1244, 2022.
3. F Ilie, **AC Cristescu**, Tribological Behavior of Friction Materials of a Disk-Brake Pad Braking System Affected by Structural Changes—A Review, *Materials* 15 (14), 4745, 2022.

B. Papers published in ISI-rated conferences:

1. **A.C. Cristescu**, I Filip, G Ipate, G Voicu, V Stefan, Studies and research on the tribological behavior of the braking systems of vehicles. Review, TE-RE-RD, E3S Web of Conferences 286, 03021, 2021.
2. G Ipate, F Ilie, **AC Cristescu**, Finite element 3D numerical simulation study of car braking systems and brake disc/drum–pad/shoe friction couple materials, TE-RE-RD, E3S Web of Conferences 286, 03021, 2022.
3. George Ipate, **Andreea Cătălina Cristescu**, Constantin Daniel, Cotici Neluș, Evelin Gheorghiță, Daiana Ionescu, Andrei Florin Hristache, Evaluation of the tribological behavior of a brake disc-pad friction pair using a fuzzy inference model based on an adaptive network (ANFIS), 11th International Conference on Thermal Equipment, Renewable Energy and Rural Development TE-RE-RD 2023, Bucharest – Romania, 08 June - 10 June 2023, Pending publication

C. Papers published in BDI-rated bulletins

1. **A.C. Cristescu**, F. Ilie, V Stefan, L Popa, G Ipate, G Voicu, Car braking system–general aspects in a review, Acta Technica Corviniensis-Bulletin of Engineering 15 (2), 105-110, 2022.
2. **A.C. Cristescu**, F. Filip, V Stefan, L Popa, G Ipate, G Voicu, Importance of materials used in car breaking systems–review, Acta Technica Corviniensis-Bulletin of Engineering 15 (2), 13-18, 2022.
3. **A.C. Cristescu**, F. Ilie, G. Ipate, Gh. Voicu, V. Stefan, L. Popa, C. Persu, A corelattion between the coefficient of friction and braking distance and time, ISB-INMA TEH' 2023 – International Symposium, 2023, Pending publication.
4. **A.C. Cristescu**, F. Ilie, G. Ipate, Gh. Voicu, Structural and modal analysis of car breaking systems, Scientific Bulletin – University Politehnica Bucharest, Series D, Inginerie Mecanica – Pending publication, 2023, Pending publication
5. **Andreea-Catalina Cristescu,** Filip Ilie - Influence of travel speed, time, and distance of braking on the, efficiency of a car's braking system, Preprints 2023, 2023101358. https://doi.org/10.20944/preprints202310.1358.v1

OTHER PUBLISHED WORKS

1. **Andreea Catalina Cristescu**, Cristina Covaliu, Lucretia Popa, Daniel Dumitru, Alexandra Anghelet, Study on use of typha angustifolia in waste water treatment: promising method in removal of copper ions present in aquatic solution" Jelgava, 23.-25.05.2018., pg 714-720, 2018 DOI: 10.22616/ERDev2018.17.N399.
2. **Cristescu A.C.**, Popa L., Covaliu C., Dumitru D.M., Persu C., Gheorghe G., Mircea C., Anghelet A., Aplication of nanomaterials in waste water treatment review / utilizarea nanomaterialelor in epurarea apelor uzate - review in ISB-INMA TEH' -Agricultural Engineering Journal, Bucharest 26-28 October 2017, pg.691-700, 2017.
3. **Ing. Cristescu A.C**, Ph.D Popa L., Ph. D. Stud. Ing. Stefan V., Assist.Ph.D.Rotaru Al, Ing. Anghelet A., Ph. D. Stud Zaica A, Ph. D. Stud. Zaica Al, Ph. D. Stud Gageanu „Study on new mechanized harvesting technologies in vineyards/ Studiu asupra noilor tehnologii de recoltare mecanizata in viticultura", ACTA Technica Corviniensis – Bulletin of Engineering, vol. 3, pp 39-42, 2019.
4. **Ing. Cristescu Andreea-Catalina**, Dr. Ing.Popa Lucretia, Drd. Ing. Stefan Vasilica, Ing. Anghelet Alexandra „Modeling, simulation and study of loads and deformations in traction devices", TE-RE-RD Conference 31 May-02 June, 2018.
5. Lucretia Popa, Luciana Dudici, Ancuta Nedelcu, **Andreea Catalina Cristescu**, Daniel Dumitru, „Kinetostatic analysis of ratchet mechanism that acts on conveyor of manure spreading machine", engineering for rural development", Jelgava, 23.-25.05.2018, pg 57-63, DOI: 10.22616/ERDev2018.17.N070.

6. Mircea C., Sorică E., Sorică C., Brăcăcescu C., Zaica Al., Zaica A., Anghelet A., Dumitru D.M., **Cristescu A.C.**, Considerations on the importance of liquorice active principles / Consideratii privind importanța principiilor active ale lemnului dulce, in ISB-INMA TEH' - Agricultural and mechanical engineering, Bucharest 26-28 October 2017, pg. 247-250.
7. Persu C., Ivancu B., Voicu Gh., Gheorghe G., Cujbescu D., Sorica E, **Cristescu A.**, Grigore I., Mircea C., Nitu M., "Determining the damping coefficient for the suspending elastic elements from a vibrating feeder", in ISB-INMA TEH' - Agricultural and mechanical engineering, Bucharest 26-28 October 2017, pg. 353-356.
8. Anghelet A., Nedelcu A., Mircea C., Zaica A., Dumitru I., Dumitru D., **Cristescu A.**, Modern technologies of algae biomass using for obtaining alternative fuels, in Annals of the Faculty of Engineering Hunedoara, vol 16, nr 4, pg 183-187, 2018.
9. Mircea I.D., Vlăduţ V., Matache M., Persu C., Voicea I., Cujbescu D., Ungureanu N., Dumitru I., Oprescu M., Iuga D., **Cristescu A.C.**, "Experimental research on coupling devices" in ISB-INMA TEH' - Agricultural and mechanical engineering, Bucharest 26-28 October 2017, pg.763 -768.
10. Dumitru D. M., Popa L., **Cristescu A.C.**, Costin M., Anghelet A., Sorica C.,Sorica E., "Zootechnical constructions. Shelter systems for cattle. Review", ISB-INMA TEH' - Agricultural and mechanical engineering, Bucharest 26-28 October 2017, pg.791-796, 2017.
11. Dumitru I., Voicea I., Găgeanu I., Cujbescu D., Persu C., Vlăduţ V., Bolintinenu Gh., Matache M., Ungureanu N., Zăbavă B., Dincă M., Boruz S., Iuga D., **Cristescu A**. "Technical considerations regarding to harvesting potatoes and carrots equipment", in Analele Universităţii din Craiova, seria Agricultură – Montanologie – Cadastru (Annals of the University of Craiova - Agriculture, Montanology, Cadastre Series) Vol. XLVII 2017, pag 317-323, ISSN 1841-8317, ISSN CD-ROM 2066-950X, http://anale.agro-craiova.ro/.
12. Vlăduţ D.I., Biriş S., Vlăduţ V., Persu C., Grigore I., Voicea I., Cujbescu D., Ungureanu N., Găgeanu I., Caba I., Atanasov At., Dumitru I., Oprescu M., Iuga D., **Cristescu A.C.**, „Experimental researches concerning the working process of a germinal bed preparation equipment for heavy soils / Cercetări experimentale privind procesul de lucru al unui echipament de pregătit patul germinativ pentru soluri grele", in ISB – INMA TEH' - Agricultural and mechanical engineering, Bucharest 26-28 October 2017, pg.781-790, ISSN 2537-3773.
13. Dumitru I., Persu C., Oprescu M., Cujbescu D., **Cristescu A.**,,Nitu M., Gageanu I., Biris S., Maican E., Ungureanu N., "Complex testing of protective structures of operators in an overturning incident", in ISB-INMA TEH' - Agricultural and mechanical engineering, Bucharest 26-28 October 2017, pg.891-898, ISSN 2537-3773.
14. Zaica A., Ciupercă R., Nedelcu A., Zaica Al., Popa L., Anghelet A., Ștefan V., **Cristescu A.C.**, Aspects regarding the flattened installation for the drying cereals in a wet condition / Aspecte privind instalația de aplatizat in vederea însilozării cerealelor in stare umedă, , in ISB-INMA TEH - Agricultural and mechanical engineering, Bucharest 01-03 November 2018, pg 395-400, ISSN 2344 – 4118.
15. Popa L., Moise St. I. Ștefan V., **Cristescu A.C**., Moise V., Dudici L., Rotaru A., Nedelcu L., Zaica A., Anghelet Al., Technologies and equipments for vineyards, in the context of climate change/ Tehnologii și echipamente pentru pomicultură/viticultură in contextul schimbărilor climatice, in ISB-INMA TEH - Agricultural and mechanical engineering, Bucharest 01-03 November 2018, pg 351-356, ISSN 2344 – 4118.
16. Popa L., Moise St. I., Moise V., Dudici L., Ştefan V., Rotaru A., **Cristescu A.C.**, Kinematic analysis of a folding bridge using combined transmission functions by three sectors / Analiza cinematică a unui pod rotitor utilizând funcțiile de transmitere combinate cu trei sectoare, in ISB-INMA TEH' - Agricultural and mechanical engineering, Bucharest 26-28 October 2017, pg. 411-418, ISSN 2537-3773.
17. Nedelcu A., Ciupercă R., Popa L., Ph Zaica A., Zaica Al., Anghelet A., Ștefan V., **Cristescu A.C.**, Aspects about organic waste composting in biocontainer / Aspecte privind compostarea deșeurilor organice în biocontainere, in ISB-INMA TEH' - Agricultural and mechanical engineering, Bucharest 26-28 October 2017, pg.425-430, ISSN 2537-3773.
18. Anghelet A., Nedelcu A., Zaica A., Dumitru D., **Cristescu A.**, Toma S., Echipamente tehnice pentru obtinerea materialului furajer sub forma de sroturi, in Technomarket 2018, Nr. 1 (19), pag 36-37.
19. Anghelet A., Ştefan V. Popa L., Nedelcu A., **Cristescu A.C.**, Dudici L., Ciuperca R., Zaica A., Anghelet A., Mechanization technologies for vineyard pruning / Tehnologii de mecanizare pentru taierile in plantatiile de vita de vie, in ISB-INMA TEH' - Agricultural Engineering Journal, Bucharest 26-28 October 2017, pg. 811-817, ISSN 2537-3773.
20. Anghelet A., Maican E., Nedelcu A., Zaica A., **Cristescu A.**, Stefan V., aspects regarding the analysis of the stress in front loader components / Aspecte privind analiza solicitarilor din componentele încărcătorului frontal, in ISB-INMA TEH - Agricultural and mechanical engineering, Bucharest 01-03 November 2018, pg 351-356, ISSN 2344 – 4118.